Inorganic Chemistry

Article

pubs.acs.org/IC

Palladium-Catalyzed Direct Arylation of Luminescent Bis-Cyclometalated Iridium(III) Complexes Incorporating *C^N*- or *O^O*-Coordinating Thiophene-Based Ligands: an Efficient Method for Color Tuning

Kassem Beydoun,[†,‡] Moussa Zaarour,[†,‡] J. A. Gareth Williams,[§] Thierry Roisnel,[⊥] Vincent Dorcet,[⊥] Aurélien Planchat,[#] Abdou Boucekkine,[†] Denis Jacquemin,*[,#,∥] Henri Doucet,*[,†] and Véronique Guerchais*[,†]

[†]UMR-CNRS 6226, Institut des Sciences Chimiques de Rennes, Université de Rennes 1, Campus de Beaulieu, 35042 Rennes, France

[§]Department of Chemistry, Durham University, South Road, Durham, United Kingdom DH1 3LE

[⊥]Centre de Diffractométrie X, UMR-CNRS 6226, Institut des Sciences Chimiques de Rennes, Campus de Beaulieu, 35042 Rennes, France

[#]UMR CNRS-6230, CEISAM, Université de Nantes, 2 rue de la Houssinière, 44322 Nantes Cedex 3, France

[∥]Institut Universitaire de France, 103 boulevard St Michel, 75005 Paris Cedex 5, France

Supporting Information

ABSTRACT: We report the palladium-catalyzed direct 5-arylation of both metalated and nonmetalated thiophene moieties of iridium complexes **2**, **3**, and **4** with aryl halides via C−H bond functionalization. This method opens new routes to varieties of Ir complexes in only one step, allowing easy modification of the nature of the ligand. The photophysical properties of the new functionalized complexes have been studied by means of absorption and emission spectroscopy. The extension of the π-conjugated system induces a bathochromic and hyperchromic shift of the absorption spectra, an effect reproduced by first principle calculations. Indeed, the bathochromic shifts are related to a more delocalized nature of the excited-states. All complexes are photoluminescent in the red region of the spectrum. This study establishes that arylation of the thienyl ring affects strongly the electronic properties of the resulting complexes, even when the thienyl ring is remote and not directly metalated to the iridium center, as in the thienyltrifluoroacetonate complex **4**.

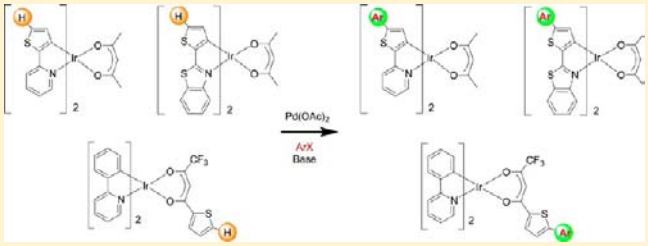

INTRODUCTION

Cross-coupling reactions between organometallic reagents and aryl halides, such as the Stille, Suzuki or Negishi reactions, have emerged as powerful synthetic tools for the construction of carbon−carbon bonds. Such catalytic coupling processes have been applied to a wide scope of substrates to produce compounds for biological science or materials chemistry.[1] One of the major drawbacks of these methodologies is the need to prepare organometallic reagents. During the past decade, synthetic efforts shifted toward the palladium-catalyzed direct arylation of (hetero)aromatic substrates via C−H bond activation, for which there is no need to prepare organometallic derivatives.[2−5] Moreover, these couplings avoid the stoichiometric formation of metallic side products and the related undesired contamination that could be potentially harmful for applications in biology or materials science.

Ir(III) complexes of metalated arylpyridines including 2,2′-thienyl-pyridine, such as tris- and bis-cyclometalated iridium complexes of the form $Ir(C^{\wedge}N)_3$ and $Ir(C^{\wedge}N)_2(L^{\wedge}X)$, respectively, are well-known for the strong room-temperature phosphorescence they often display.[6−8] An attractive feature of this class of complexes is that tuning of the emission color can be readily achieved by chemical modification of the $(C^{\wedge}N)$ ligand. Yet this approach requires access to a variety of substituted chelating ligands, and no straightforward and versatile general route is currently available. While relevant proligands are accessible using Stille, Negishi, or Suzuki cross-coupling reactions,[1,9] subsequent access to the bis- or tris-cyclometalated complexes might be incompatible with the use of ligands bearing reactive functional groups, owing to the harsh conditions required for the formation of the complexes, particularly the *tris*-cyclometalates. Therefore, in order to improve the synthetic accessibility of such luminescent complexes, we have developed a direct and selective method for the functionalization of *tris*-cyclometalated iridium com-

Received: May 21, 2013
Published: October 14, 2013

   dx.doi.org/10.1021/ic401208p | *Inorg. Chem.* 2013, 52, 12416−12428

plexes using the so-called "direct arylation" strategy involving regioselective C−H bond functionalization of the thiophene ligands. We showed that the charge-neutral iridium(III) complex Ir(*C*^*N*-thpy)$_3$, **1**, bearing 2,2′-thienylpyridine (thpy) ligands can be arylated at the C-5 position of the thienyl rings with a variety of electron-deficient aryl bromides, via a C−H bond functionalization (Scheme 1).[10] We demonstrated that this catalytic method is a powerful tool for tuning the emission wavelengths by changing the nature of the appended aryl group.

Scheme 1. Pd-Catalyzed Direct Arylation of the *tris*-Cyclometalated Complex Ir(*C*^*N*-thpy)$_3$, 1

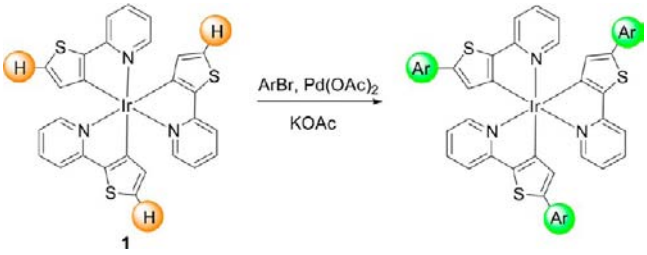

Within this context, it is of particular interest to extend this methodology to other Ir(III) complexes, and, more specifically, to the related bis-cyclometalated complexes[8] whose emitting properties remain intriguing. The Pd-catalyzed direct arylation of complexes incorporating the 2,2′-thienylpyridine (thpy) or 2,2′-thienylbenzothiazole (thbt) ligands (complexes **2** and **3**, Figure 1, the ancillary ligand being acetylacetonate) has never been described yet and is clearly worthy of study.

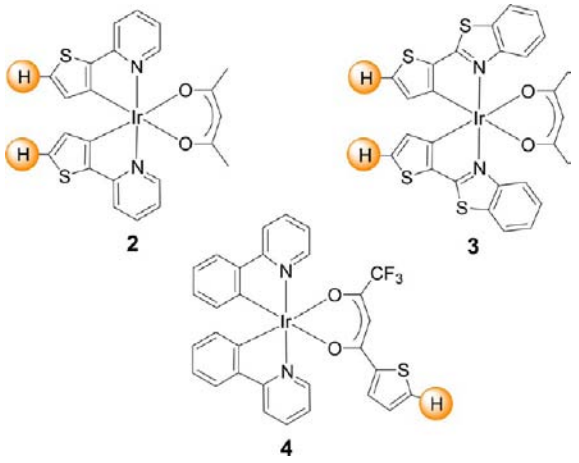

Figure 1. Chemical structures of the *bis*-cyclometalated heteroleptic Ir(III) complexes: Ir(*C*^*N*-thpy)$_2$(*O*^*O*-acac), **2**, Ir(*C*^*N*-thbt)$_2$(*O*^*O*-acac), **3** and Ir(*C*^*N*-ppy)$_2$(*O*^*O*-tta), **4**.

Although the so-called "ancillary" ligand in Ir(*C*^*N*)$_2$(*O*^*O*) complexes often plays no significant role in the electronic excited state(s), there are exceptions, e.g., when the *O*^*O* ligand incorporates an aryl substituent with extended conjugation.[11] This prompted us to investigate the Pd-arylation of the iridium complex Ir(*C*^*N*-ppy)$_2$(*O*^*O*-tta), **4**[12] (ppyH = 2-phenylpyridine) bearing the thienyl-based thienyltrifluoroacetonate (tta) as coligand. The palladium-catalyzed direct arylation of the non-cyclometalated thienyl ring of the ancillary ligand would provide new insights into the generality of the catalytic C−H bond activation reaction.

Here, we report the Pd-catalyzed regioselective C5-arylation of the metalated thienyl ring(s) of complexes **2** and **3**, to produce mono- and bis-arylated Ir(III) complexes. We have also achieved, under quite mild reaction conditions, the Pd-catalyzed direct arylation of a thiophene unit of the ancillary ligand of **4**. This method represents an efficient and direct—only one step—route to new families of arylated heteroleptic Ir(III) complexes. The influence of the chemical modification of the (*C*^*N*) or (*O*^*O*) ligand on the photophysical properties of the resulting complexes will be presented and interpreted with the help of time-dependent density functional theory (TD-DFT) calculations. The influence of the location and nature of the incorporated aryl group is also discussed.

RESULTS AND DISCUSSION

The precursor complexes **2** and **3** were prepared according to published procedures.[8a] Complex **4** was prepared from [Ir(*C*^*N*-ppy)$_2$$\mu$-Cl]$_2$ in the presence of 4,4,4-trifluoro-1-thiophen-2-ylbutane-1,3-dione following the same method reported for **2** and **3**. First, we attempted to promote the coupling of complex **2** with 4-bromobenzonitrile (4 equiv.) in the presence of Pd(OAc)$_2$ as the catalyst and KOAc as the base (Scheme 2). Such phosphine-free reaction conditions,

Scheme 2. Pd-Catalyzed Direct Arylation of the Thiophene Unit(s) of 2 with Various Aryl Bromides

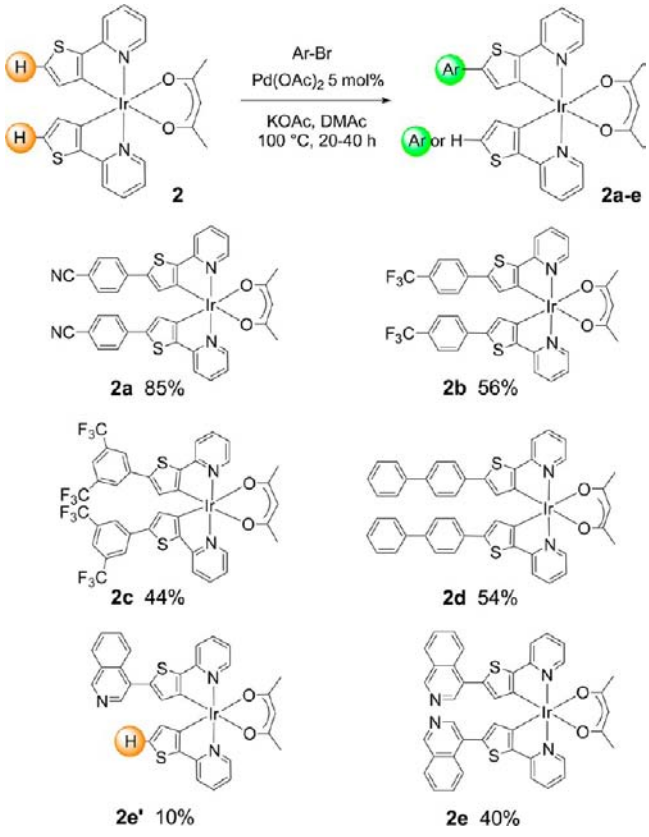

previously operative on various heteroarene derivatives,[5f,10] rule out the possible decomposition of the iridium complexes by ligand exchange with phosphines. Under these conditions, at 150 °C the formation of the desired diarylated complex **2a** was observed along with some decomposition of the iridium complex. This outcome might originate in the partial decoordination of the acetylacetonate ligand at this temper-

dx.doi.org/10.1021/ic401208p | *Inorg. Chem.* 2013, 52, 12416−12428

ature. Notably, by performing the reaction at 100 °C, a clean reaction was observed and the diarylated iridium complex **2a** was isolated in 85% yield (Scheme 2). In the course of this reaction, no significant amount of the monoarylated iridium complex was detected.

Then, the scope of this reaction was examined using a variety of other (hetero)aryl bromides (Scheme 2). Electron-deficient para-substituted aryl bromides, 4-(trifluoromethyl)-bromobenzene and 3,5-bis(trifluoromethyl)bromobenzene, gave the desired 5-arylated thiophene complexes **2b** and **2c** in 56% and 44% yield, respectively. From 4-bromobiphenyl, the complex **2d** was obtained in 54% yield. Next, the reactivity of 4-bromoisoquinoline for the coupling with **2** was examined. The use of this heterocycle led to the formation of a mixture of the mono- and diarylated iridium complexes; separation by column chromatography afforded both complexes **2e′** (10%) and **2e** (40%) in pure form.

We also examined the reactivity of the iridium complex **3** bearing two 2-thienylbenzothiazole ligands (Scheme 3). In all

Scheme 3. Pd-Catalyzed Direct Arylation of the Thiophene Unit(s) of 3 with Various Aryl Bromides

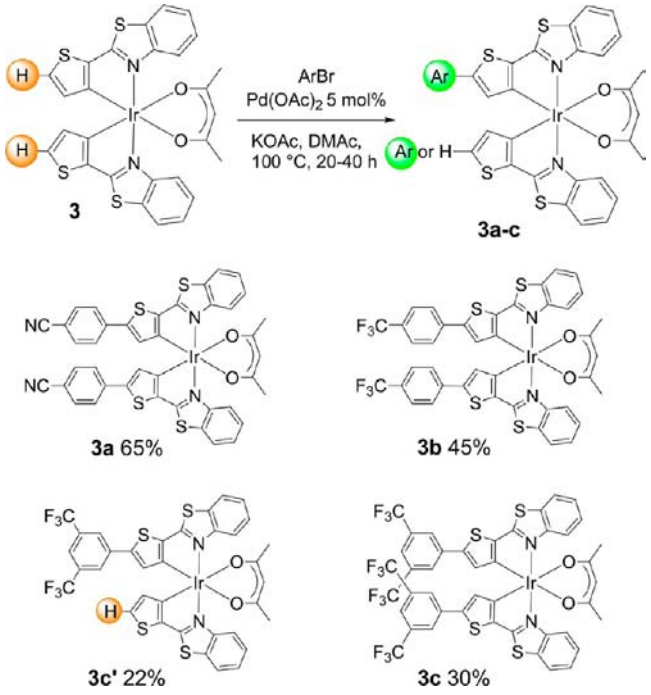

cases, lower yields for direct arylation of **3** were obtained than with **2**. Using similar reaction conditions, we found that **3** can be di-arylated with 4-bromobenzonitrile or 4-(trifluoromethyl)-bromobenzene to give **3a** and **3b** in 65% and 45% yield, respectively. This lower reactivity was confirmed by the arylation of **3** with 3,5-bis(trifluoromethyl)bromobenzene which led to the formation of a mixture of the monoarylated complex **3c′** and diarylated complex **3c** in 22% and 30% yield, respectively. All complexes **3a**–**c** were purified by column chromatography.

Single crystals of complexes **3a** and **3c** suitable for X-ray crystallographic studies were obtained by the slow diffusion of pentane vapor into a concentrated solution of the complex in CH_2Cl_2. The perspective view is depicted in Figures 2 and 3. Selected bond lengths and angles are listed in Tables 1 and 2 respectively. It is noted that the iridium centers adopt a distorted octahedral coordination geometry with *cis*-O,O, *cis*-C,C, and *trans*-N,N chelate disposition. The bond lengths of **3a** and **3c** were found to be in the same range as those reported for the iridium bis-thienylquinoline (thq) complex Ir(*C*^*N*-thq)$_2$(acac).[13] They have slightly larger C–Ir–C angles (96.21° (**3a**) and 96.3° (**3c**)) compared to that of Ir(*C*^*N*-thq)$_2$(acac) (94.1°).

Then, we investigated the reactivity of the thiophene unit of complex **4** using again a set of aryl halides (Scheme 4). First we employed 4-bromobenzonitrile as the coupling partner and 5 mol % Pd(OAc)$_2$ catalyst. The desired benzonitrile-substituted product **4a** was isolated in 57% yield. The arylation was completely regioselective in favor of the C5 arylation of the thiophene unit. The electron-deficient aryl bromides, 4-(trifluoromethyl)-bromobenzene and 3,5-bis(trifluoromethyl)-bromobenzene, led to the target complexes **4b** and **4c**.

In contrast to the series **2** and **3**, incorporation of arenes bearing electron-donating substituents was effective in this case. Our initial attempt at coupling **4** with 4-bromoanisole led to the formation of only a trace amount of the desired product **4d**. This result was not surprising because the oxidative addition of 4-bromoanisole using Pd(OAc)$_2$ catalyst is sluggish. By contrast, the use of 4-iodoanisole gave the expected product **4d** in 71% yield. The direct use of unprotected anilines in such couplings is of interest since it would allow simple further transformation without the protection/deprotection sequence of the NH_2 function. From 4-iodoaniline and 5 mol % Pd(OAc)$_2$, **4e** was obtained in a very good yield of 70%. Finally, we employed 2-chloro-4-iodoaniline as the coupling partner, the target complex **4f** being isolated in 42% yield. It should be noted that no cleavage of the C–Cl bond was observed in the course of this reaction allowing further transformations either at NH_2 or Cl positions of the benzene ring.

The electrochemical behavior of selected Ir(III) metal complexes, series **2** and **4** used as representative examples, was investigated by cyclic voltammetry using ferrocene as the internal standard (see Table S1 in the Supporting Information). The arylated complexes of series **2**, all undergo a quasi-reversible one-electron oxidation (see Table S1 in the Supporting Information), as observed for the parent Ir(*C*^*N*-thpy)$_2$(*O*^*O*-acac), **2**.[8b] There is some variation in the oxidation potential with substituent (0.29–0.82 V), although no clear trend can be discerned.

The behavior of the complexes of series **4** is more revealing. All of these complexes display a quasi-reversible oxidation wave and a quasi-reversible reduction within the solvent window (see Table S1 in the Supporting Information). That a reduction process is observed for series **4** but not for series **2** suggests that the reduction in the former may occur primarily on the low-lying π^* orbitals of the ancillary tta ligand, which is more electron-deficient than the corresponding acac ligand of series **2**. The reduction processes of all the arylated complexes of series **4** are cathodically shifted relative to the parent complex **4** itself, consistent with the introduction of π-donating aryl substituents. Notably, the most strongly donating system (the anilino group of **4e**) leads to the most negative reduction potential, consistent with the tta ligand being the site of the reduction. Meanwhile, the oxidation potentials of the arylated derivatives (in the region 0.47–0.55 V) are shifted by about 0.5 V to lower values compared to **4** itself, suggesting that the first oxidation in these complexes may be associated more with the functionalized tta ligand. These conclusions are to a significant extent borne out by the TD-DFT calculations discussed below.

dx.doi.org/10.1021/ic401208p | *Inorg. Chem.* 2013, 52, 12416–12428

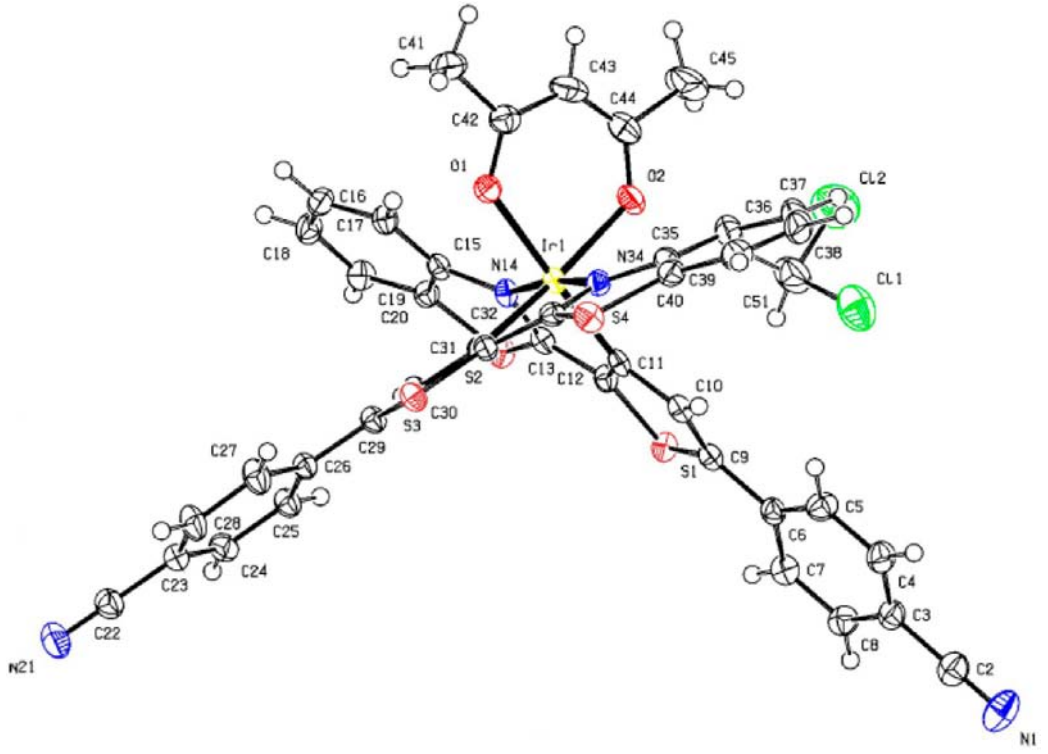

Figure 2. Perspective view of the molecular structure of complex **3a**.

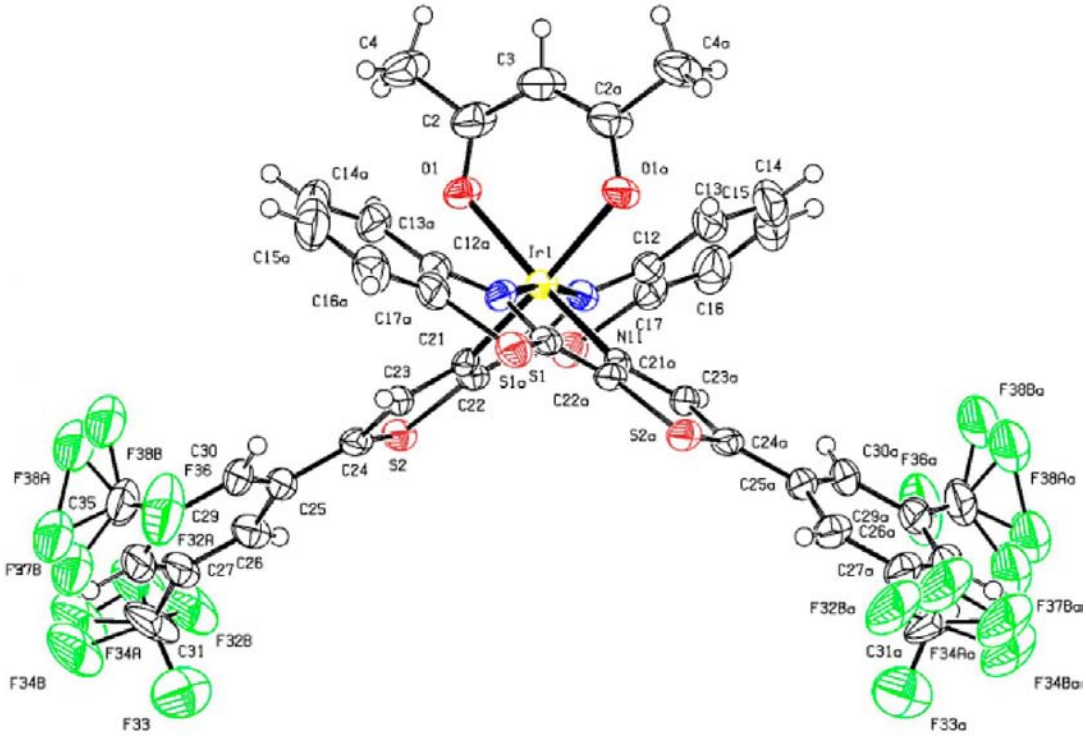

Figure 3. Perspective view of the molecular structure of complex **3c**.

Absorption Studies. The photophysical properties of the new Ir(III) complexes were investigated by absorption spectroscopy in CH_2Cl_2 solution at room temperature and the data are listed in Table 3. The absorption spectrum of the starting thienylpyridine complex **2** and the arylated derivatives **2** and **2a**–**d** are presented in Figure 4a. Compared to **2**, the electronic spectrum of complex **2a** incorporating a benzonitrile group is red-shifted and presents larger molar extinction coefficients. The spectrum displays broad and intense bands in the 300–400 nm region, which can be attributed to ^{1}IL($\pi\rightarrow\pi^*$) transitions of the ($C^\wedge N$) ligands. The moderately intense band in the visible region is shifted to longer wavelength by ca. 30 nm (ca. 1000 cm^{-1}) compared to **2**. This band, which extends up to 550 nm, can be assigned to a blend of IL($\pi\rightarrow\pi^*$) and

dx.doi.org/10.1021/ic401208p | *Inorg. Chem.* 2013, 52, 12416–12428

Table 1. Selected Bond Lengths of Complexes 3a and 3c

complex **3a**	bond length (Å)	complex **3c**	bond length (Å)
Ir−C31	1.988(2)	Ir−C21	1.990(4)
Ir−C11	1.992(2)	Ir−C21a	1.990(4)
Ir−N34	2.052(2)	Ir−N11	2.064(4)
Ir−N14	2.055(2)	Ir−N11a	2.064(4)
Ir−O1	2.1195(17)	Ir−O1	2.152(3)
Ir−O2	2.1379(17)	Ir−O1a	2.152(3)

Table 2. Selected Bond Angles of Complexes 3a and 3c

complex **3a**	bond angle (deg)	complex **3c**	bond angle (deg)
C31−Ir1−C11	96.21(9)	C21a−Ir1−C21	96.3(2)
C31−Ir1−N34	79.73(9)	C21a−Ir1−N11	93.19(16)
C11−Ir1−N34	96.51(9)	C21−Ir1−N11)	79.92(16)
C31−Ir1−N14	93.68(9)	C21a−Ir1-N11a	79.92(16)
C11−Ir1−N14	79.76(9)	C21−Ir1−N11a	93.18(16)
N34−Ir1−N14	172.10(7)	N11−Ir1−N11a	169.73(19)
C31−Ir1−O1	86.79(8)	C21a−Ir1-O1	174.15(13)
C11−Ir1−O1	176.53(7)	C21−Ir1−O1	88.53(14)
N34−Ir1−O1	85.74(7)	N11−Ir1−O1	90.88(13)
N14−Ir1−O1	98.32(7)	N11a−Ir1-O1	96.58(13)
C31−Ir1−O2	174.72(8)	C21a−Ir1-O1a	88.53(14)
C11−Ir1−O2	88.87(8)	C21−Ir1−O1a	174.15(13)
N34−Ir1−O2	98.29(8)	N11−Ir1−O1a	96.58(13)
N14−Ir1−O2	88.65(7)	N11a−Ir1−O1a	90.89(13)
O1 −Ir1−O2	88.18(7)	O1−Ir1−O1a	86.83(16)

Scheme 4. Pd-Catalyzed Direct Arylation of the Thiophene Unit of 4 with Various Aryl Halides

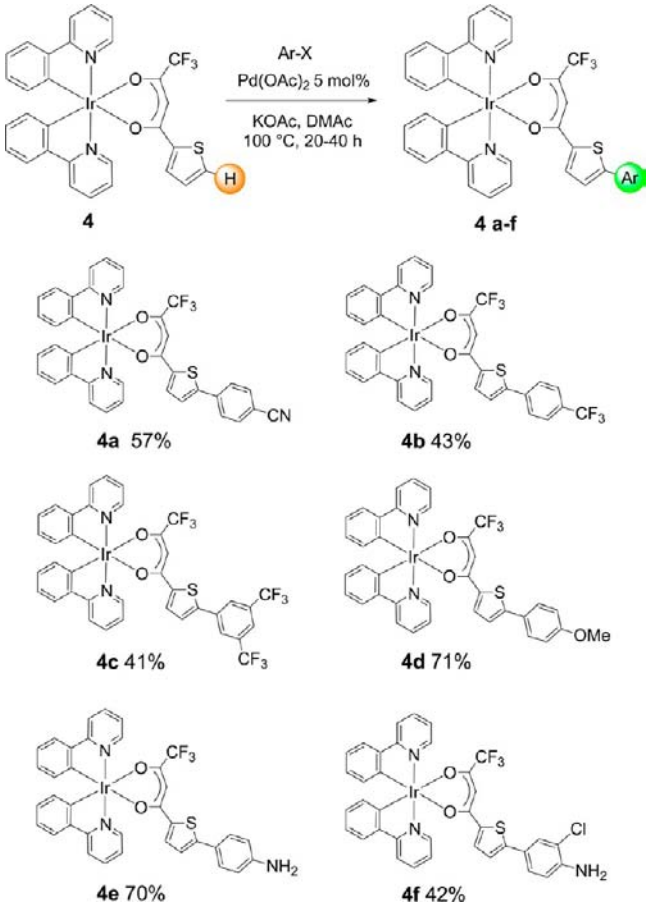

MLCT ($d\pi(Ir)\rightarrow\pi^*(C\text{^}N)$) transitions (see TD-DFT calculations below). For the broad absorption in the 300−400 nm domain, the red-shift versus the parent complex **2** is slightly larger for **2a** than for the CF_3-substituted complexes (**2b** and **2c**), probably as a result of lower-energy charge-transfer transitions reflecting the presence of the more strongly electron-withdrawing cyano group. It may be noted that complexes **2b** and **2c** show nearly identical absorption spectra, showing that the electronic effect of the substitution by a CF_3 group in the 4-position of the appended phenyl group is comparable to that of disubstitution at the 3- and 5-positions.

The absorption spectra of the thienylbenzothiazole complex **3** and the arylated derivatives **3a−c** and **3c′** are shown in Figure 4b and data are summarized in Table 3. The spectra of **3a−c** exhibit three well-resolved bands. The intense absorption bands in the UV region at 300−400 nm could be attributed to a mixture of $^1IL(\pi\rightarrow\pi^*)$ transitions of the *C^N* ligands and MLCT transition. The bands in the visible region at 400−600 nm are ascribed to spin-allowed ^{1}MLCT with possible contribution of ^{3}MLCT ($d\pi(Ir)\rightarrow\pi^*(C\text{^}N)$) transitions (vide infra). As above, for all diarylated species, the molar extinction coefficients increase as a result of the extension of the π-conjugation on the *C^N* ligand.

Interestingly, having available the mono- and the diarylated complexes **3c′** and **3c** bearing one or two 3,5-bis-CF_3-phenyl groups, respectively, we can see how the absorption properties are affected by the number of incorporated aryl groups. The intense absorption band in the UV region is located for the monoarylated complex **3c′** at 339 nm (ε = 26 600 M^{-1} cm^{-1}) while that of the diarylated species **3c** is found at 360 nm (ε = 41 900 M^{-1} cm^{-1}) with a higher molar extinction coefficient. The bands in the visible region appear at ca. 430 nm. The lowest-energy band remains almost unchanged. The behavior of **3a** and **3b** are comparable to each other, and are in line with that of **3c**. As for the series of thpy complexes, these bands are attributed to a mixture of $^1IL(\pi\rightarrow\pi^*)$ transitions of the ($C\text{^}N$) ligands and MLCT transitions. The replacement of the pyridine ligand of **2a−c** by the benzothiazole in **3a−c** induces a relatively small bathochromic shift (∼15 nm).

The family of phenylpyridine-based complexes **4a−f** containing an arylated thiophene-based ancillary ligand can be divided into two groups: complexes **4a−c** incorporating electron-acceptor end groups and complexes **4d−f** incorporating electron-donating end groups. (Figure 5, Table 3). The arylated derivatives within each group present similar absorption profiles to one another. The UV−visible absorption spectra of complexes **4a−c** incorporating a phenyl ring substituted with 4-CF_3, 3,5-di-CF_3 and 4-CN substituents show two well-resolved bands at 350−357 and 393 nm. As observed for the arylated cyclometalated thiophene complexes (series **2** and **3**), there is a hyperchromic shift of the whole spectrum within the series, compared to the starting non-arylated complex **4**. A very broad and intense band was observed in the absorption spectra of complexes **4d−f** incorporating aryl groups with donor end groups, λ_{max} for which increased in the order **4d** (400 nm) < **4f** (415 nm) < **4e** (420 nm). The absorption spectrum of complex **4e** incorporating the 4-aniline group, the best donating group, is the most red-shifted. In all cases, the presence of these appended aryl groups made the resulting complexes stronger absorbers in the visible range.

TD-DFT Studies. We have modeled the spectra of selected derivatives (complexes **2**, **2a**, **2e**, **2e′**, and **3**, **3a**, **3c**, **3c′**) using

dx.doi.org/10.1021/ic401208p | *Inorg. Chem.* 2013, 52, 12416−12428

Table 3. Photophysical Data of the Investigated Ir(III) Complexes

	$\lambda_{absorption}$ (nm) (ε [$M^{-1}cm^{-1}$])[a]	λ_{em} (nm)[b]	Φ (%)[e]	τ (ns)[b]
2	282 (24900), 317 (21200), 366 (16400), 414 (4700), 464 (5000)	565, 609[c]	31	3400
2a	252 (19600), 321 (32200), 360 (39300), 410 (15600), 488 (8900)	682, 774[c]	0.8	830
2b	250 (20700), 313 (38100), 349 (39300), 407 (12000), 488 (9100)	660, 672[c]	1.9	1100
2c	250 (21200), 313 (40300), 348 (41500), 407 (11700), 488 (9500)	665, 730[c]	1.6	1100
2d	273 (25300), 323 (38900), 358 (39500), 488(9400)	670, 733[c]	1.4	1600
3	276 (18200), 332 (26400), 407 (9300), 450 (8100), 488 (7300)	600, 651, 455[c]	25	2300
3a	283 (22200), 368 (36800), 442 (17900), 507 (10300)	712, 782[c]	0.4	260
3b	278 (21300), 358 (34600), 426 (17200), 507 (9800)	693,763[c]	2.0	420
3c	280 (23400), 360 (41900), 430 (18100), 495 (12200)	697, 770[c]	0.8	340
3c′	280 (17500), 339 (26600), 440 (10100), 507 (6000)	697, 770[c]	1.1	300
4	265 (44500), 303 (27800), 331 (21300), 363 (15000), 450 (3800)	532[d]	0.19	1300
4a	266 (27200), 357 (19400), 393 (17400)	517, 546, 587[d]	0.045	1600
4b	265 (33000), 355 (22200), 392 (19800)	512, 547, 588[d]	0.034	1300
4c	266 (37000), 350 (25600), 393 (19700)	*f*	*f*	*f*
4d	262 (44000), 400 (33000)	492[d]	0.16	1.5
4e	260 (39000), 420 (27800)	563[d]	0.63	2.8
4f	260 (31700), 300 (19000), 415 (24000)	546[d]	0.87	2.7

[a]Values refer to solutions in CH_2Cl_2 at 298 K, except where indicated otherwise. [b]In degassed CH_2Cl_2 solutions. [c]λ_{exc} = 455 nm. [d]λ_{exc} = 430 nm. [e]$Ru(bpy)_3Cl_2$ was used as the standard (Φ = 0.028 in air-equilibrated water[18]). [f]The emission from this complex was too weak to obtain reliable data.

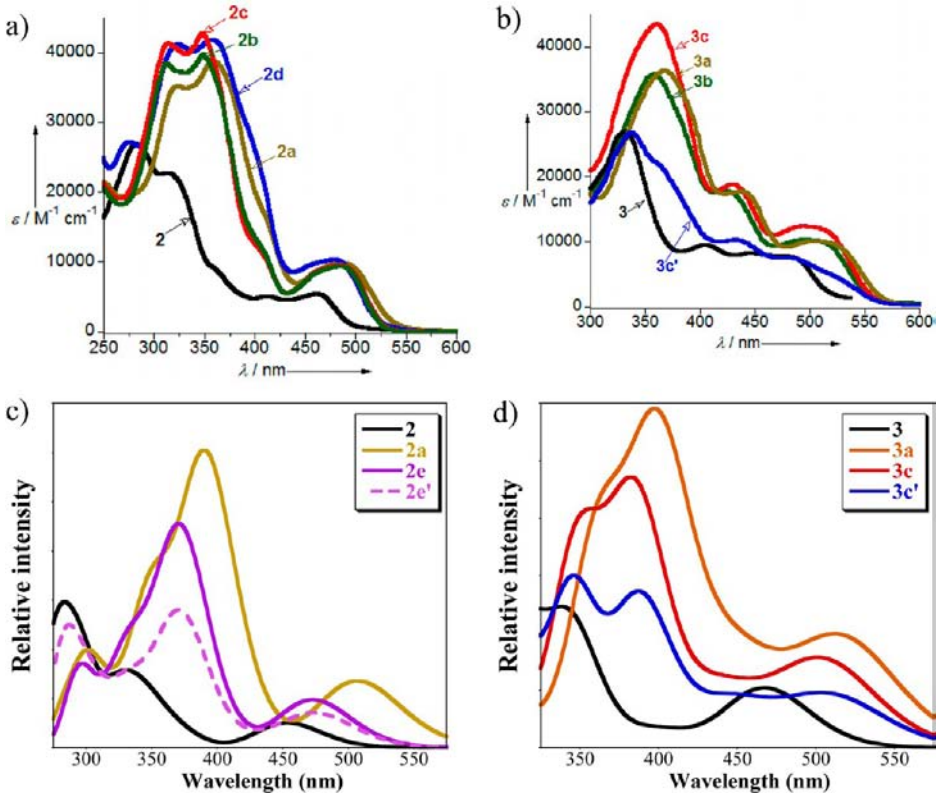

Figure 4. UV−vis absorption spectra (CH_2Cl_2, 298 K) for (a) Ir(*C*^*N*-thpy-Ar)$_2$(*O*^*O*-acac), **2**, and **2a**−**d**; (b) Ir(*C*^*N*-thbt-Ar)$_2$(*O*^*O*-acac), **3**, **3a**−**c**, and Ir(*C*^*N*-thbt-Ar)(*C*^*N*-thbt)(*O*^*O*-acac) **3c**′. Simulated absorption spectra for (c) **2**, **2a**, **2e**, and **2e**′; (d) **3**, **3a**, **3c** and **3c**′. A convoluting Gaussian with fwhm of 0.35 eV has been used.

first-principle TD-DFT simulations coupled with continuum environmental effects. We have selected the M06 functional to perform our calculations, as this functional accurately reproduces the available XRD parameters (see computational details), is adequate for organometallics,[14] and has been shown to be efficient for simulating absorption spectra.[15] Computational details are given in the Experimental Section. For **2**, **2a**, **2e**, and **2e**′ the simulated spectra are displayed in Figure 4c and the qualitative match with the experimental spectra in Figure 4a is satisfactory. Indeed, adding additional aromatic rings induces a joint bathochromic/hyperchromic shift of the ca. 450 and ca. 350 nm bands, their respective positions being reproduced within the expected TD-DFT accuracy. More precisely, in **2**, the lowest-energy absorption is computed at 454 nm (464 nm experimentally) and mainly corresponds to a HOMO−LUMO transition, that is to a dπ(Ir)→π*(*C*^*N*) transition, as expected,

dx.doi.org/10.1021/ic401208p | *Inorg. Chem.* 2013, 52, 12416−12428

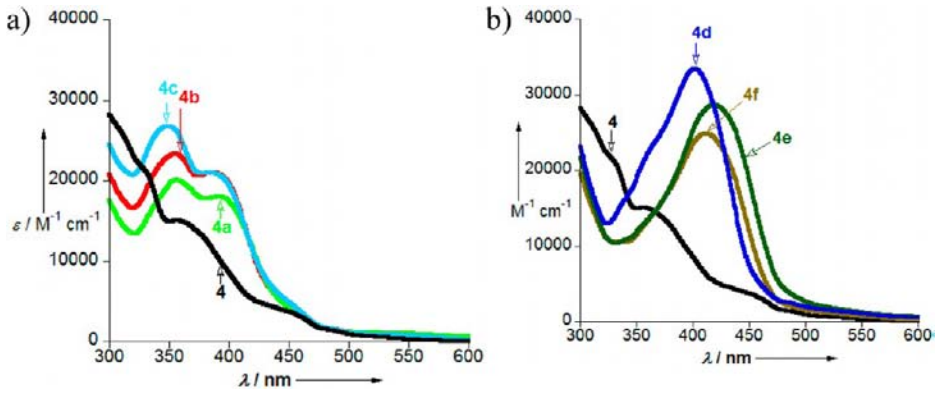

Figure 5. Absorption spectra (CH_2Cl_2, 298 K) of Ir(*C*^*N*-ppy)$_2$(*O*^*O*-tta-Ar) **a)** **4** and **4a**–**c**, (b) **4** and **4d**–**f**.

though one should note that the HOMO is partly delocalized on the thiophene rings. The intense band in the UV spectra of **2** is computed to peak near 330 nm, which is consistent with experimental trends. The largest contribution of the most intense vertical transition corresponding to this band can be ascribed to an individual ^{1}IL($\pi\rightarrow\pi^*$) transition, but smaller contributions incorporating the metal orbitals still play a role. For **2a**, theory foresees a long wavelength band at 506 nm (488 nm in the experiment) whereas the most intense band appears at 390 nm (360 nm in the experiment). The analysis is less straightforward than for **2**, because each peak encompasses a larger number of individual vertical transitions, which cannot be ascribed to single occupied/virtual MO pairs. Therefore, we have used density difference plots rather than orbitals to analyze the electronic reorganization (see Figure 6). One

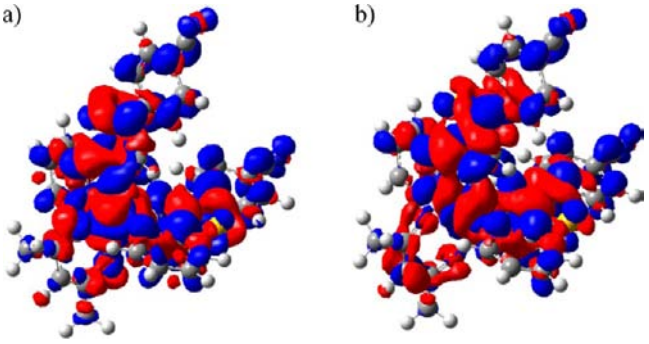

Figure 6. Density difference plots for the vertical transitions dominating the (a) 506 nm and (b) 390 nm absorption bands of **2a**. The blue (red) zones indicate increase (decrease) of the electronic density upon transition.

notices a CT character that is induced by the cyano groups that gain density upon electronic transition. We also underline that the electronic reorganization upon absorption takes place on the entire molecule (but the acac part).

Let us now turn to **3** and three of its analogues, namely **3a**, **3c**, and **3c**′. Results are displayed in Figure 4d, and the computed trends qualitatively match experiment. Indeed, when going from **2** to **3**, one notices a +14 nm shift accompanied by a +50% increase of the intensity of the longest wavelength band, and theory foresees a +14 nm (658 cm^{-1}) displacement (from 454 to 468 nm) together with a doubling of the oscillator strength. From the density difference plots for the longest wavelength (Figure 7), it can be seen that the nature of the excited state does not change significantly between **2** and **3**,

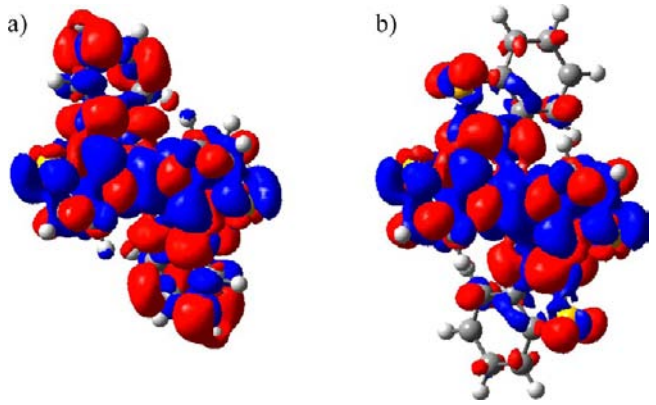

Figure 7. Density difference plots for the first dipole-allowed vertical transitions of (a) **2** and (b) **3**. See caption of Figure 6 for more details. Both molecules are oriented with the acac group on the back and the metal at the center.

although in **3**, the six-member rings do not undergo electronic reorganization upon transition. Complexes **3a** and **3c** present similar density difference plots (not shown) and positions of the main bands. The lowest energy band of **3a** is predicted at 512 nm, in very good agreement with experiment at 507 nm and is more intense than that of **3**. Again, these bands and the more intense transition at ca. 350–400 nm, all correspond to a blend between MLCT and IL transitions, the bathochromic/hyperchromic displacement within the series of arylated complex **3a**–**c** being related to the more delocalized nature of the excited states. As expected from its structure, **3c**′ presents an intermediate behavior between **3** and **3c**, in both theory and experiment.

Emission Studies. All complexes are photoluminescent at room temperature in fluid solution (CH_2Cl_2, 298 K). The emission spectra of complexes **2** and **2a**–**d** are presented in Figure 8a and data are summarized in Table 3. The nonsubstituted complex **2** was found to present a structured emission band at room temperature at 565 nm originating primarily from ^{3}IL (π–π^*).[7d] The arylated derivatives **2a**–**d** show structured emission bands with similar vibrational structuring to that of **2** (Δ = 1340–1740 cm^{-1}). The emission wavelengths lie in the range of 660–680 nm, red-shifted by ~100–110 nm (~2780 cm^{-1}) compared to **2**. This trend is likely to be the result of the extension of the π-conjugated system. This is confirmed by theoretical calculations that show that the spin density of the triplet state is delocalized over the entire molecules in **2a** except on the acac (Figure 9). A

dx.doi.org/10.1021/ic401208p | *Inorg. Chem.* 2013, 52, 12416–12428

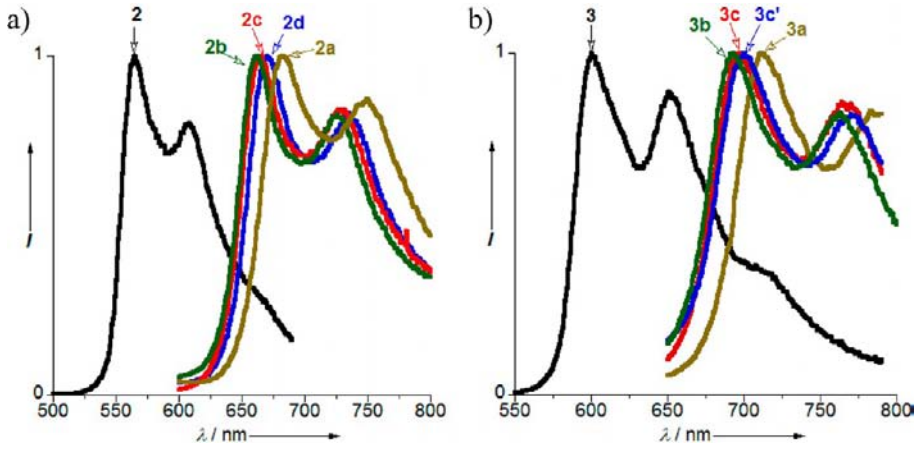

Figure 8. Emission spectra (CH_2Cl_2, 298 K) of a) Ir(*C^N*-thpy-Ar)$_2$(*ÔO-acac*), **2** and **2a−d** Ir(*C^N*-thbt)$_2$(*O^O-acac*) **3**, Ir(*C^N*-thbt-Ar)$_2$(*O^O-acac*) **3a−c** and Ir(*C^N*-thbt)(*C^N*-thbt-Ar) (*O^O-acac*) **3c′**.

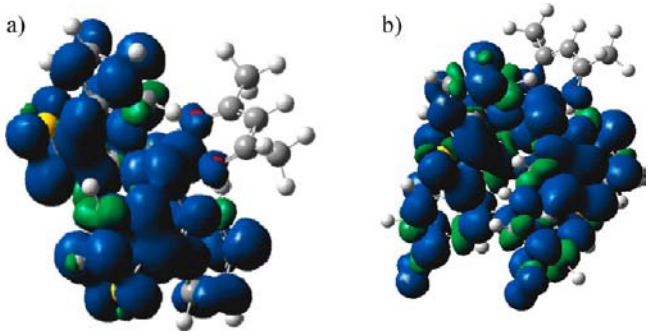

Figure 9. Computed spin density difference plots for the triplet state of (a) **2** and (b) **2a**.

progressive red-shift was observed upon introducing an accepting end-group, the cyanophenyl complex **2a** showed the largest red-shift (λ = 682 nm). On the basis of the shape of the emission bands and their vibrational structuring compared to **2**, the emission of complexes **2a−d** could be assigned to a primarily ligand centered excited state ^{3}IL (π−π*). The arylated complexes **2a−d** have low photoluminescence quantum yields (Φ) between 0.8 and 1.9% and lifetimes (τ) ranging from 0.83 to 1.6 μs which are shorter than that of **2**. If we assume that the emissive excited state is formed with unitary efficiency in each case (a reasonable assumption given that the excitation spectra match well the absorption spectra), then an estimate of the radiative, k_r, and nonradiative, Σk_{nr}, rate constants can be made as follows: $k_r = \Phi/\tau$ and $\Sigma k_{nr} = (\tau^{-1} - k_r)$. Such an analysis reveals that in the arylated complexes, the rate constant of nonradiative decay is increased by around an order of magnitude (e.g., comparing **2** and **2a**, $\Sigma k_{nr} = 2.0 \times 10^5$ s^{-1} and 1.2×10^6 s^{-1}, respectively), whereas the rate constant of emission is decreased by an order of magnitude (e.g., again comparing **2** and **2a**, $k_r = 9.1 \times 10^4$ s^{-1} and 9.6×10^3 s^{-1}, respectively). The latter observation could be attributed to the decreasing influence of the spin−orbit coupling effect of the metal, as the excited state becomes more delocalized over the more extended ligand, as has been observed previously with complexes of Ir(III), Pt(II) and Re(I) with extended ligands.[8d,16] This is confirmed by the calculations showing that the Ir(III) represents an average of 17% and 6% in the three highest occupied α MO of the triplet of **2** and **2a**, respectively. Alternatively, it may be due to a larger energy gap between the T_1 excited state and the higher-lying ^{1}MLCT state(s) with which the triplet state must mix in order for triplet emission to be induced.[17] Indeed, it can be seen clearly from the data in Table 3 that the arylation has a greater stabilizing effect on the triplet states than on the lowest-energy singlet states: the emission energies drop by around 3000 cm^{-1}, whereas the corresponding change in the absorption energies is only around 1000 cm^{-1}. This observation suggests that the S−T gaps are increased in the arylated complexes compared to the parent complex. Meanwhile, the faster nonradiative decay may be associated with more efficient coupling of the electronic excited state with vibrations in the ligand.

The emission spectra of the benzothiazole complexes **3**, **3a−c**, and **3c′** are presented in Figure 8b and data are summarized in Table 3. The parent complex **3** presents a structured emission at 600 nm from a ^{3}IL (π−π*) excited state[7d] (ϕ = 25%, τ = 2.3 μs). Similar to the arylated thienylpyridine family, the arylated benzothiazole derivatives **3a−c** display red-shifted emission profiles compared to the precursor complex **3** ($\Delta \approx$ 90−110 nm or ∼2400 cm^{-1}) with similar band shape and vibrational structuring originating primarily from ^{3}IL (π−π)* excited state. Interestingly, it was found that both the mono- and diarylated complexes **3c′** and **3c**, respectively emit exactly at the same wavelength (697 nm) with similar emission lifetimes and quantum yields to one another even though they have different absorption profiles. This observation indicates that both complexes emit from the same lowest energy excited state which is likely to be located on the substituted ligand. For **3**, **3a**, and **3c**, we optimized the geometry of the triplet emitting state with DFT. Relatively small geometrical variations compared to the ground singlet state have been found, e.g. in **3a**, the Ir−C, Ir−N, and Ir−O distances go from 1.981, 2.072, and 2.159 Å (singlet) to 1.952, 2.068, and 2.167 Å (triplet), respectively. Consistent with these limited variations, the triplet energies computed in the adiabatic (using the difference of free energies between the two states) and vertical (performing TD-DFT calculations on the ground-state structures) limits are consistent. Indeed, using the adiabatic (vertical) scheme, we compute a triplet state energy at 570 (582), 691 (685), and 641 (662) nm, for **3**, **3a**, and **3c**, respectively. It is noticeable that the strong bathochromic shift upon extension of the conjugated path is well restored by theory.

The emission data of complexes **4** and **4a−e** are summarized in Table 3 and the spectra are presented in Figure 10. The tta

dx.doi.org/10.1021/ic401208p | *Inorg. Chem.* 2013, 52, 12416−12428

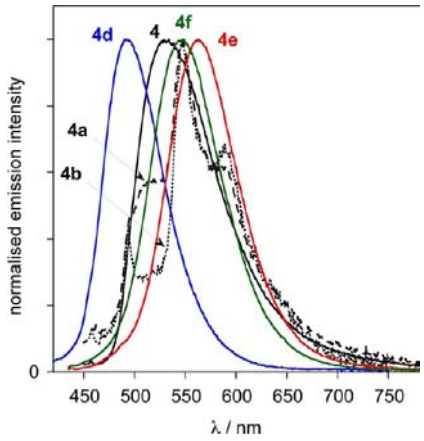

Figure 10. Normalized emission spectra (CH_2Cl_2, 298 K) of Ir(*C*^*N*-ppy)$_2$(*O*^*O*-tta) **4** and Ir(*C*^*N*-ppy)$_2$(*O*^*O*-tta-Ar) **4a,b,d-f** (The "spike" at 494 nm in the very weak spectrum of **4b** is a C−H Raman band of the solvent).

complex **4** (λ_{max} = 532 nm) shows a much lower phosphorescence quantum yield (ϕ = 0.19%) than the parent acac complex Ir(*C*^*N*-ppy)$_2$(*O*^*O*-acac).[11] The arylated derivatives **4a** and **4b** incorporating phenyl rings substituted by electron-withdrawing groups (*p*-CN and *p*-CF_3 respectively) emit only very weakly indeed, around an order of magnitude lower again than **4**. They display structured emission profiles with the highest-energy band at ∼517 nm, perhaps indicative of a more ligand-localized excited state, as the degree of conjugation in the functionalized tta increases. The lifetimes of around 1−2 μs are, however, consistent with the emission having a triplet-state origin. The emission of complex **4c** was too weak to obtain reliable data.

In contrast, complexes **4d−f**, incorporating electron-rich aryl substituents, display unstructured spectra, and the quantum yields are an order of magnitude higher. Although their spectra appear similar in form to the emission spectrum of the parent compound **4**, a striking difference emerges when the emission decay kinetics are examined. These three complexes emit with lifetimes of around 2 ns, namely 3 orders of magnitude shorter than that observed for **4** and **4a**,**b**, and their emission is insensitive to oxygen. We were unable to detect any significant long-lived emission for these complexes in solution at room temperature. Thus it appears that the introduction of electron-rich aryl pendants into the tta unit promotes fluorescence from the singlet state of the functionalized tta. Presumably, as the conjugation in this unit is extended and the energy level of the frontier orbitals associated with it increases, the spin−orbit coupling influence of the metal ion diminishes, to the extent that the S→T intersystem crossing rate is reduced to a value where fluorescence can compete. Moreover, the lower effect of the metal will serve to reduce the rate constant of phosphorescence from the triplet state, so that it will be less able to compete with nonradiative decay pathways, making any phosphorescence essentially negligible at room temperature. Some precedent for such an effect comes from a study of oligo(thienyl)pyridine ligands with iridium(III) and platinum(II).[8d] Thus, while the complexes of thienylpyridine itself were strongly phosphorescent, the appendage of one (for Pt) or two (for Ir) additional thienyl rings onto the metalated thiophene ring led to the appearance of fluorescence from the oligothiophene unit, with a concomitant reduction in phosphorescence intensity. It is notable that in the present case, the effect is observed only with the electron-donating substituents, which are more comparable to thiophene in terms of "electron-richness". A related phenomenon has also been reported for a series of osmium(II) complexes incorporating β-diketonate ligands that feature increasingly conjugated aryl substituents (phenyl, naphthyl, anthryl and pyrenyl).[16]

Consistently with the above interpretation, the TD-DFT calculations highlight that the triplet state localization is strongly modified as a function of the appended ligand. As can be seen in Figure 11, the triplet of complex **4d** is mainly localized on the functionalized tta ligand, with little participation of the metal.

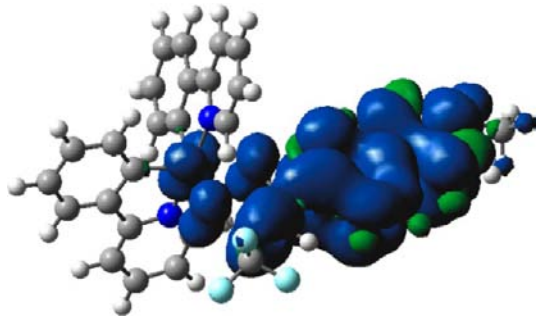

Figure 11. Spin density representation of the triplet state complex **4d**.

CONCLUSION

In summary, cyclometalated 2,2″-thienylpyridine or 2-thienylbenzothiazole ligands coordinated to iridium(III) and also a thiophene-based ancillary iridium-ligand can be directly arylated with a panel of aryl halides using $Pd(OAc)_2$ catalyst. In all cases, the thiophene ring is regioselectively arylated at the C-5 position. A variety of heteroleptic bis-cyclometalated iridium complexes have been synthesized and fully characterized. We demonstrate that the photophysical properties of bis-cyclometalated Ir(III) complexes can be easily modulated by changing the extension of π-conjugation on the *C*^*N* ligand, the nature of the substituent on the aryl group, and the nature of ancillary ligand at the iridium center with the help of Pd-catalyzed C−H bond functionalization. Indeed, the TD-DFT calculations show that the excited state is delocalized over the entire ligand(s) and to present a mixed CT, MLCT and IL character allowing fine-tuning of the properties. Moreover, with regards to environmental considerations, the advantages of such a procedure for the modification of coordinated ligands, which produces only limited amounts of inert waste (side products limited to the formation of acetic acid and potassium bromide), will become increasingly important, including for future industrial processes.

EXPERIMENTAL SECTION

General. All catalytic reactions were performed in Schlenk tubes under argon using analytical grade dimethylacetamide (DMAc) and potassium acetate (99%+). Commercial aryl halides and heteroaromatic derivatives were used without purification. Flash chromatography was performed on silica gel (230−400 mesh). ^{1}H (500, 400, or 300 MHz) and ^{13}C (125, 100, or 75 MHz) NMR spectra were recorded in $CDCl_3$ solution at 298 K. Chemical shifts are reported in ppm relative to $CDCl_3$ (^{1}H: 7.29 and ^{13}C: 77.0).

UV−Visible and Emission Spectroscopy. UV−visible absorption spectra were recorded using a UVIKON 9413, analytikjena SPECORD 205 or Biotek Instruments XS spectrophotometer using

quartz cuvettes of 1 cm path length. Steady-state luminescence spectra were measured using a Jobin Yvon FluoroMax-2 fitted with a red-sensitive Hamamatsu R928 photomultiplier tube, or an Edinburgh Instruments spectrometer FLSP920—Steady State spectrometer. The spectra were corrected for the wavelength dependence of the detector, and the quoted emission maxima refer to the values after correction. Luminescence quantum yields were determined using $[Ru(bpy)_3]Cl_2$ in air-equilibrated water as the standard, for which Φ_{lum} = 0.028;[18] estimated uncertainty in Φ_{lum} is ±20% or better. Lifetimes were obtained either by time-correlated single-photon counting following excitation at 374 nm with a laser diode and detection of the light emitted at right angles using an R928 photomultiplier tube, after passage through a monochromator, or using an Edinburgh Instruments LP920 laser flash photolysis spectrometerwith the 355 nm-third harmonic of a nanosecond-pulsed Nd:YAG laser (Continuum Surelite II, Excel Technology). The Levenberg—Marquardt algorithm was applied for nonlinear least-squares fitting (tail fit) as implemented in the L900 software (Edinburgh instrument).

X-ray Structures of Complexes 3a and 3c. X-ray diffraction data were collected at 150 K using an APEXII, Bruker-AXS diffractometer with CCD rotation images, thin slices (CCD plate detector). Data were processed with the use of SAINT integration program[19a] and absorption correction was performed by the multiscan method with SADABS.[19b] The structure was solved with the program SIR97[20] and refined by full-matrix least-squares based on F^2 using SHELXL-97.[21] Iridium atoms and many non-hydrogen atoms were located according to direct methods. The positions of other non-hydrogen atoms were found after successful refinements and difference Fourier maps analysis. In the final stage of refinement, all non-hydrogen atoms were refined anisotropically. Crystal data and a summary of the data collection and refinement details are given in Table 4. The supplementary crystallographic data for this paper can be obtained free of charge from the Cambridge Crystallographic Data Centre via www.ccdc.cam. ac.uk/data_request/cif. Deposition numbers: CCDC 923704 and 923705

Table 4. Crystal Data and Summary of Data Collection and Refinement for Complex 3a and 3c

	3a	3c
empirical formula	C_{42} H_{27} Cl_2 Ir N_4 O_2 S_4	C_{43} H_{23} F_{12} Ir N_2 O_2 S_4
formula weight	1011.02	1148.07
crystal size (mm)	0.48 × 0.36 × 0.1	0.44 × 0.28 × 0.13
T (K)	150	150
cryst syst	Triclinic	Monoclinic
space group	P-1	C 2/c
a, b, c (Å)	12.4712(8), 12.6001(7), 16.7180(9)	17.4704(10), 19.5830(10), 14.9601(7)
α, β, γ (deg)	112.030(2), 106.407(3), 111.969(3)	90, 111.644(2), 90
V (Å ^{3})	1966.4(2)	4757.3(4)
Z	2	4
ρ calcd (mg/m^{-3})	1.708	1.603
μ (mm^{-1})	3.786	3.066
F (000)	996	2240
θ range (deg)	3.06 −27.48	2.93−27.48
index ranges	$-16 \le h \le 16$, $-16 \le k \le 16$, $-20 \le l \le 21$	$-22 \le h \le 22$, $-25 \le k \le 21$, $-10 \le l \le 18$
total reflns	32082	16066
data/restraints/params	8925/0/498	5316/0/291
GOF on F^2	1.048	1.085
R_1, wR_2 ($I > 2s(I)$)	0.0218, 0.0536	0.0381, 0.0936
R_1, wR_2 (all data)	0.0250, 0.0550	0.0529, 0.0983
largest diff. peak, hole (e Å^{-3})	0.861, −0.648	1.141, −0.608

Synthesis of Ir(ppy)$_2$(tta) (4). In a Schlenk tube, under argon atmosphere, the chloro-bridged dimer $Ir(C^N\text{-}2\text{-}ppy)_2(\mu\text{-}Cl)]_2$ (0.289 g, 0.27 mmol), 4,4,4-trifluoro-1-(2-thienyl)-1,3-butanedione (0.155 g, 0.70 mmol), and K_2CO_3 (0.386 g, 2.80 mmol) were introduced into 10 mL of 2-ethoxyethanol. The reaction mixture was heated at 80 °C for 24 h, quenched by 10 mL of distilled water and the precipitate was decanted by centrifugation. The product was then washed with water, ethanol, and diethyl ether to afford **4** in 72% (0.301 g) isolated yield as an orange powder. ^{1}H NMR (400 MHz, CD_2Cl_2): δ 8.55 (ddd, J = 5.8, 1.6, and 0.8 Hz, 1H), 8.52 (ddd, J = 5.7, 1.6, and 0.8 Hz, 1H), 7.95 (td, J = 7.0 and 0.9 Hz, 2H), 7.85 (td, J = 8.0 and 1.6 Hz, 1H), 7.84 (td, J = 8.0 and 1.6 Hz, 1H), 7.71 (dd, J = 3.9 and 1.2 Hz, 1H), 7.68—7.66 (m, 1H), 7.66—7.64 (m, 1H), 7.59 (dd, J = 5.0 and 1.1 Hz, 1H), 7.25 (ddd, J = 7.3, 5.8, and 1.4 Hz, 1H), 7.20 (ddd, J = 7.3, 5.8, and 1.4 Hz, 1H), 7.08 (dd, J = 5.0 and 3.8 Hz, 1H), 6.94 (m, 2H), 6.82—6.74 (m, 2H), 6.32 (ddd, J = 7.6, 1.2, and 0.5 Hz, 1H), 6.29 (s, 1H), 6.27 (ddd, J = 7.7, 1.2, and 0.5 Hz, 1H). ^{13}C NMR (100 MHz, CD_2Cl_2): δ 176.4, 168.0, 167.91, 147.92, 145.7, 145.0, 144.5, 143.9, 137.7, 133.1, 131.6, 129.0, 128.9, 128.4, 123.98, 123.8, 122.2, 122.1, 121.4, 121.3, 118.9, 118.7, 92.67. HRMS calcd for M$^+$ $C_{30}H_{20}F_3N_2O_2F_3SIr$ 722.08215, found: 722.0809.

General Procedure for Coupling Reactions. In a typical experiment, the reaction of the aryl bromide, iridium complex **2—4** and KOAc at 100 °C in DMAc in the presence of $Pd(OAc)_2$, under argon affords the coupling product after evaporation of the solvent and filtration on silica gel (pentane/ether).

*Diarylation of **2** with 4-Bromobenzonitrile (**2a**).* The reaction of 4-bromobenzonitrile (0.146 g, 0.8 mmol), **2** (0.122 g, 0.2 mmol), and KOAc (0.079 g, 0.8 mmol) with $Pd(OAc)_2$ (0.002 g, 0.01 mmol) in DMAc (3 mL) at 100 °C during 40 h affords the product **2a** in 85% (0.138 g) isolated yield as a brown solid. ^{1}H NMR (500 MHz, $CDCl_3$): δ 8.42 (d, J = 5.4 Hz, 2H), 7.72 (t, J = 7.8 Hz, 2H), 7.55 (d, J = 7.8 Hz, 2H), 7.51—7.40 (m, 8H), 7.06 (t, J = 6.6 Hz, 2H), 6.50 (s, 2H), 5.32 (s, 1H), 1.87 (s, 6H). ^{13}C NMR (125 MHz, $CDCl_3$): δ 184.7, 164.2, 149.3, 148.5, 144.7, 138.8, 138.7, 137.7, 132.2, 130.2, 125.8, 119.2, 118.9, 117.0, 109.8, 100.8, 28.5. HRMS calcd for M$^+$ $C_{37}H_{25}N_4O_2S_2Ir$ 814.1043, found 814.1042.

*Diarylation of **2** with 4-Trifluoromethylbromobenzene (**2b**).* The reaction of 4-trifluoromethylbromobenzene (0.180 g, 0.8 mmol), **2** (0.122 g, 0.2 mmol), and KOAc (0.079 g, 0.8 mmol) with $Pd(OAc)_2$ (0.002 g, 0.01 mmol) in DMAc (3 mL) at 100 °C during 40 h affords the product **2b** in 56% (0.100 g) isolated yield as a brown solid. ^{1}H NMR (500 MHz, $CDCl_3$): δ 8.41 (d, J = 5.4 Hz, 2H), 7.71(t, J = 7.4 Hz, 2H), 7.60—7.48 (m, 10H), 7.03 (t, J = 7.4 Hz, 2H), 6.49 (s, 2H), 5.30 (s, 1H), 1.88 (s, 6H). ^{13}C NMR (125 MHz, $CDCl_3$): δ 184.7, 164.7, 149.7, 148.6, 145.5, 138.1, 137.7, 137.6, 129.8, 128.8 (q, J = 32.8 Hz), 126.3 (q, J = 271 Hz), 125.9, 125.5 (q, J = 3.7 Hz), 118.8, 117.5, 100.8, 28.6. HRMS calcd for M$^+$ $C_{37}H_{25}IrN_2O_2F_6S_2$ 900.0886, found 900.0890.

*Diarylation of **2** with 3,5-Bis(trifluoromethyl)bromobenzene (**2c**).* The reaction of 3,5-bis(trifluoromethyl)bromobenzene (0.234 g, 0.8 mmol), **2** (0.122 g, 0.2 mmol), and KOAc (0.079 g, 0.8 mmol) with $Pd(OAc)_2$ (0.002 g, 0.01 mmol) in DMAc (3 mL) at 100 °C during 40 h affords the product **2c** in 44% (0.092 g) isolated yield as a brown solid. ^{1}H NMR (500 MHz, $CDCl_3$): δ 8.42 (d, J = 5.3 Hz, 2H), 7.85 (s, 4H), 7.76 (t, J = 7.8 Hz, 2H), 7.67 (s, 2H), 7.61 (d, J = 7.8 Hz, 2H), 7.09 (t, J = 7.2 Hz, 2H), 6.51 (s, 2H), 5.32 (s, 1H), 1.88 (s, 6H). ^{13}C NMR (125 MHz, $CDCl_3$): δ 184.8, 164.3, 149.4, 148.6, 143.5, 138.6, 138.0, 136.8, 131.9 (q, J = 32.8 Hz), 130.4, 125.6 (m), 123.2 (q, J = 271 Hz), 120.3 (m), 119.4, 117.8, 100.8, 28.6. HRMS calcd for M$^+$ $C_{39}H_{23}N_2O_2F_{12}S_2Ir$ 1036.0633, found 1036.0634.

*Diarylation of **2** with 4-Phenylbromobenzene (**2d**).* The reaction of 4-bromobiphenyl (0.186 g, 0.8 mmol), **2** (0.122 g, 0.2 mmol), and KOAc (0.079 g, 0.8 mmol) with $Pd(OAc)_2$ (0.002 g, 0.01 mmol) in DMAc (3 mL) at 100 °C during 40 h affords the product **2d** in 54% (0.098 g) isolated yield as a brown solid. ^{1}H NMR (500 MHz, DMSO): δ 8.36 (d, J = 5.4 Hz, 2H), 7.89 (t, J = 7.5 Hz, 2H), 7.71 (d, J = 7.5 Hz, 2H), 7.68—7.62 (m, 8H), 7.53 (d, J = 8.4 Hz, 2H), 7.48—7.42 (m, 4H) 7.38—7.33 (m, 4H), 7.24 (t, J = 7.2 Hz, 2H), 6.40 (s, 2H), 5.33 (s, 1H), 1.80 (s, 6H). ^{13}C NMR (125 MHz, DMSO): δ

184.6, 164.0, 145.3, 148.8, 146.0, 139.8, 139.7, 139.1, 136.2, 133.1, 129.4, 128.6, 128.0, 127.7, 126.8, 126.3, 120.2, 117.9, 105.0, 28.5. HRMS calcd for M^+ $C_{47}H_{35}N_2O_2S_2Ir$ 916.1764, found 916.1761.

*Arylation of **2** with 4-Bromoisoquinoline (**2e** and **2e′**).* The reaction of 4-bromoisoquinoline (0.166 g, 0.8 mmol), **2** (0.122 g, 0.2 mmol), and KOAc (0.079 g, 0.8 mmol) with $Pd(OAc)_2$ (0.002 g, 0.01 mmol) in DMAc (3 mL) at 100 °C during 40 h affords a mixture of the products **2e′** (monoarylation) in 10% (0.015 g) isolated yield and **2e** (diarylation) in 40% (0.070 g) isolated yield as brown solids. Complex **2e′**: ^{1}H NMR (500 MHz, $CDCl_3$): δ 9.16 (s, 1H), 8.56 (s, 1H), 8.42 (d, J = 5.5 Hz, 1H), 8.40 (d, J = 5.5 Hz, 1H), 8.15 (d, J = 8.0 Hz, 1H), 7.96 (d, J = 8.0 Hz, 1H), 7.68−7.63 (m, 2H), 7.61 (t, J = 7.4 Hz, 2H), 7.55 (d, J = 8.0 Hz, 1H), 7.51 (d, J = 8.0 Hz, 1H), 7.25 (d, J = 4.7 Hz, 1H), 6.99 (t, J = 5.8 Hz, 1H), 6.94 (t, J = 5.8 Hz, 1H), 6.34 (s, 1H), 6.25 (d, J = 4.7 Hz, 1H), 5.31 (s, 1H), 1.91 (s, 3H), 1.87 (s, 3H). ^{13}C NMR (125 MHz, $CDCl_3$): δ 184.6. 184.5, 165.2, 164.9, 151.5, 149.6, 148.6, 148.4, 148.2, 143.1, 140.6, 137.7, 137.4, 137.3, 135.8, 133.5, 132.5, 131.8, 130.5, 128.2, 128.0, 127.7, 127.1, 125.5, 124.9, 118.5, 118.4, 117.2, 117.1, 100.7, 28.6, 28.5. HRMS calcd for M^+ $C_{32}H_{24}N_3O_2S_2Ir$ 739.0934, found 739.0933. Complex **2e**: ^{1}H NMR (500 MHz, $CDCl_3$): δ 9.15 (s, 2H), 8.57 (s, 2H), 8.44 (d, J = 5.8 Hz, 2H), 8.13 (d, J = 7.8 Hz, 2H), 7.96 (d, J = 7.8 Hz, 2H), 7.66−7.51 (m, 8H), 6.98 (t, J = 5.8 Hz, 2H), 6.40 (s, 2H), 5.37 (s, 1H), 1.94 (s, 6H). ^{13}C NMR (125 MHz, $CDCl_3$): δ 184.8, 174.3, 164.9, 152.0, 149.2, 148.7, 143.0, 140.7, 137.8, 137.6, 134.1, 133.6, 130.7, 128.3, 127.8, 127.2, 124.9, 118.7, 117.3, 100.9, 28.7. HRMS calcd for M^+ $C_{41}H_{29}N_4O_2S_2Ir$ 866.1356, found 866.1359.

*Diarylation of **3** with 4-Bromobenzonitrile (**3a**).* The reaction of 4-bromobenzonitrile (0.109 g, 0.6 mmol), **3** (0.108 g, 0.15 mmol), and KOAc (0.059 g, 0.6 mmol) with $Pd(OAc)_2$ (0.0016 g, 0.007 mmol) in DMAc (3 mL) at 100 °C during 40 h affords the product **3a** in 65% (0.090 g) isolated yield as a brown solid. ^{1}H NMR (500 MHz, $CDCl_3$): δ 7.98 (d, J = 8.3 Hz, 2H), 7.91 (d, J = 8.3 Hz, 2H), 7.52 (d, J = 8.1 Hz, 4H), 7.50−7.43 (m, 8H), 6.52 (s, 2H), 5.23 (s, 1H), 1.85 (s, 6H). ^{13}C NMR (125 MHz, $CDCl_3$): δ 185.8, 172.7, 156.9, 150.9, 148.8, 138.2, 134.6, 132.4, 131.6, 131.5, 127.7, 126.6, 125.5, 124.6, 122.5, 118.8, 110.9, 101.9, 28.2. HRMS calcd for M^+Na^+ $C_{41}H_{25}N_4O_2NaS_4Ir$ 949.0382, found 949.0378.

*Diarylation of **3** with 4-Trifluoromethylbromobenzene (**3b**).* The reaction of 4-trifluoromethylbromobenzene (0.135 g, 0.6 mmol), **3** (0.108 g, 0.15 mmol), and KOAc (0.059 g, 0.6 mmol) with $Pd(OAc)_2$ (0.0016 g, 0.007 mmol) in DMAc (3 mL) at 100 °C during 40 h affords the product **3b** in 45% (0.069 g) isolated yield as a brown solid. ^{1}H NMR (400 MHz, $CDCl_3$): δ 7.99 (d, J = 8.0 Hz, 2H), 7.90 (d, J = 8.0 Hz, 2H), 7.54−7.48 (m, 8H), 7.47−7.41 (m, 4H), 6.50 (s, 2H), 5.23 (s, 1H), 1.86 (s, 6H). ^{13}C NMR (100 MHz, $CDCl_3$): δ 185.8, 172.7, 157.3, 150.9, 149.5, 137.3, 133.7, 131.6, 131.1, 129.8 (q, J = 32 Hz), 127.6, 126.5, 125.6 (q, J = 3.7 Hz), 124.4, 122.4, 118.4, 101.8, 28.2. HRMS calcd for M^+Na^+ $C_{41}H_{25}IrN_2O_2F_6S_4$ 1035.0224, found 1035.0223.

*Arylation of **3** with 3,5-Bis(trifluoromethyl)bromobenzene (**3c** and **3c′**).* The reaction of 3,5-bis(trifluoromethyl)bromobenzene (0.175 g, 0.6 mmol), **3** (0.108 g, 0.15 mmol), and KOAc (0.059 g, 0.6 mmol) with $Pd(OAc)_2$ (0.0016 g, 0.007 mmol) in DMAc (3 mL) at 100 °C during 40 h affords a mixture of the products **3c′** (monoarylation) in 22% (0.031 g) isolated yield and **3c** (diarylation) in 30% (0.051 g) isolated yield as brown solids. Complex **3c′**: ^{1}H NMR (500 MHz, $CDCl_3$): δ 8.01−7.95 (m, 2H), 7.91−7.85 (m, 2H), 7.80 (s, 2H), 7.68 (s, 1H), 7.48−7.39 (m, 4H), 7.29 (d, J = 4.6 Hz, 1H), 6.51 (s, 1H), 6.23 (d, J = 4.6 Hz, 1H), 5.21 (s, 1H), 1.85 (s, 3H), 1.83 (s, 3H). ^{13}C NMR (125 MHz, $CDCl_3$): δ 185.7, 185.6, 173.7, 172.6, 157.4, 155.8, 151.0, 150.9, 147.2, 136.2, 134.3, 133.4, 132.3, 132.2, 132.1 (q, J = 32 Hz), 131.9, 131.7, 131.5, 127.5, 127.4, 126.2 (q, J = 3.6 Hz), 124.5, 124.2, 124.1 (q, J = 273.0 Hz), 122.5, 122.3, 121.0 (m), 118.9, 118.5, 101.8, 28.2, 28.1. HRMS calcd for M^+ $C_{35}H_{21}N_2O_2F_6NaS_4Ir$ 958.9911, found 958.9902. Complex **3c**: ^{1}H NMR (500 MHz, $CDCl_3$): δ 7.99 (d, J = 8.2 Hz, 2H), 7.92 (d, J = 8.2 Hz, 2H), 7.81 (s, 4H), 7.69 (s, 2H), 7.49−7.43 (m, 4H), 6.53 (s, 2H), 5.23 (s, 1H), 1.86 (s, 6H). ^{13}C NMR (125 MHz, $CDCl_3$): δ 185.9, 172.7, 156.8, 150.8, 147.3, 136.2, 134.5, 132.1 (q, J = 33 Hz), 131.8, 131.7, 127.7, 126.2 (q, J = 3.8 Hz), 124.7, 124.2 (q, J = 272 Hz), 122.6, 121.1 (m), 118.8, 101.8, 28.1. HRMS calcd for M^+ $C_{43}H_{23}N_2O_2F_{12}S_4Ir$ 1148.0075, found 1148.0075.

*Arylation of **4** with 4-Bromobenzonitrile (**4a**).* The reaction of 4-bromobenzonitrile (0.055 g, 0.3 mmol), **4** (0.108 g, 0.15 mmol), and KOAc (0.030 g, 0.3 mmol) with $Pd(OAc)_2$ (0.0016 g, 0.007 mmol) in DMAc (3 mL) at 100 °C during 24 h affords the product **4a** in 57% (0.071 g) isolated yield as a brown solid. ^{1}H NMR (500 MHz, $CDCl_3$): δ 8.54 (d, J = 5.8 Hz, 1H), 8.49 (d, J = 5.5 Hz, 1H), 7.90 (t, J = 7.8 Hz, 2H), 7.83−7.75 (m, 2H), 7.70−7.56 (m, 7H), 7.32 (d, J = 4.0 Hz, 1H), 7.19 (t, J = 7.2 Hz, 1H), 7.14 (t, J = 7.2 Hz, 1H), 6.91 (t, J = 7.8 Hz, 1H), 6.87 (t, J = 7.8 Hz, 1H), 6.77 (t, J = 7.2 Hz, 1H), 6. 74 (t, J = 7.2 Hz, 1H), 6.32 (d, J = 7.5 Hz, 1H), 6.25 (d, J = 7.5 Hz, 1H), 6.20 (s, 1H). ^{13}C NMR (125 MHz, $CDCl_3$): δ 174.9, 168.4, 168.3, 166.6 (q, J = 32 Hz), 147.9, 147.7, 147.1, 147.0, 144.8, 144.7, 144.6, 144.1, 138.0, 137.5, 133.3, 133.2, 132.8, 129.4, 129.1, 129.0, 126.2, 126.0, 123.9, 123.7, 121.8, 121.7, 121.3, 121.1, 118.7, 118.6, 118.5, 111.6, 92.4. HRMS calcd for M^+Na^+ $C_{37}H_{23}O_2N_3F_3NaSIr$ 846.0985, found 846.0988.

*Arylation of **4** with 4-Trifluoromethylbromobenzene (**4b**).* The reaction of 4-trifluoromethylbromobenzene (0.068 g, 0.3 mmol), **4** (0.108 g, 0.15 mmol), and KOAc (0.030 g, 0.3 mmol) with $Pd(OAc)_2$ (0.0016 g, 0.007 mmol) in DMAc (3 mL) at 100 °C during 24 h affords the product **4b** in 43% (0.056 g) isolated yield as a brown solid. ^{1}H NMR (500 MHz, $CDCl_3$): δ 8.54 (d, J = 5.5 Hz, 1H), 8.49 (d, J = 5.5 Hz, 1H), 7.90 (t, J = 7.8 Hz, 2H), 7.84−7.73 (m, 2H), 7.69 (d, J = 8.0 Hz, 2H), 7.64 (d, J = 4.0 Hz, 1H), 7.63−7.56 (m, 4H), 7.29 (d, J = 4.0 Hz, 1H), 7.19 (t, J = 7.2 Hz, 1H), 7.15 (t, J = 7.2 Hz, 1H), 6.91 (t, J = 7.8 Hz, 1H), 6.87 (t, J = 7.8 Hz, 1H), 6.78 (t, J = 7.2 Hz, 1H), 6.74 (t, J = 7.2 Hz, 1H), 6.33 (d, J = 7.5 Hz, 1H), 6.26 (d, J = 7.5 Hz, 1H), 6.20 (s, 1H). ^{13}C NMR (125 MHz, $CDCl_3$): δ 175.2, 168.4 (m), 166.4 (q, J = 32 Hz), 147.9, 147.8, 147.7, 146.3, 145.0, 144.8, 144.7, 144.3, 137.5, 137.1, 133.3, 133.2, 130.0 (q, J = 32.6 Hz), 129.5, 129.1, 129.0, 126.1, 126.0 (q, J = 3.7 Hz), 125.4, 123.9, 123.7, 121.9, 121.7, 121.3 (q, J = 272.0 Hz), 121.2, 121.1, 118.7, 118.5, 92.4. HRMS calcd for M^+Na^+ $C_{37}H_{23}O_2N_2F_6NaSIr$ 889.0906, found 889.0904.

*Arylation of **4** with 3,5-Bis(trifluoromethyl)bromobenzene (**4c**).* The reaction of 3,5-bis(trifluoromethyl)bromobenzene (0.088 g, 0.3 mmol), **4** (0.108 g, 0.15 mmol), and KOAc (0.030 g, 0.3 mmol) with $Pd(OAc)_2$ (0.0016 g, 0.007 mmol) in DMAc (3 mL) at 100 °C during 40 h affords the product **4c** in 41% (0.057 g) isolated yield as a brown solid. ^{1}H NMR (500 MHz, $CDCl_3$): δ 8.53 (d, J = 5.7 Hz, 1H), 8.49 (d, J = 5.7 Hz, 1H), 7.98 (s, 2H), 7.91 (d, J = 7.8 Hz, 2H), 7.83 (s, 1H), 7.82−7.75 (m, 2H), 7.66 (d, J = 4.0 Hz, 1H), 7.62 (d, J = 7.8 Hz, 1H), 7.58 (d, J = 7.8 Hz, 1H), 7.33 (d, J = 4.0 Hz, 1H), 7.20 (t, J = 7.2 Hz, 1H), 7.15 (t, J = 7.2 Hz, 1H), 6.92 (t, J = 7.2 Hz, 1H), 6.87 (t, J = 7.2 Hz, 1H), 6.79 (t, J = 7.8 Hz, 1H), 6.74 (t, J = 7.8 Hz, 1H), 6.34 (d, J = 7.8 Hz, 1H), 6.25 (d, J = 7.8 Hz, 1H), 6.20 (s, 1H). ^{13}C NMR (125 MHz, $CDCl_3$): δ 174.9, 168.4, 168.3, 166.8 (q, J = 32.1 Hz), 147.9, 147. 7, 147.2, 145.7, 144.8, 144.7, 144.6, 144.0, 137.5, 136.0, 133.3, 133.2, 132.5 (q, J = 33.5 Hz), 129.4, 129.1, 129.0, 126.2, 125.7, 125.6, 124.1, 123.9, 123.8, 123.0 (q, J = 273.0 Hz), 121.8, 121.7, 121.6 (m), 121.3, 121.3, 118.7, 118.6, 92.5. HRMS calcd for M^+Na^+ $C_{38}H_{22}O_2N_2F_9NaSIr$ 957.0780, found 957.0788.

*Arylation of **4** with 4-Iodoanisole (**4d**).* The reaction of 4-iodoanisole (0.070 g, 0.3 mmol), **4** (0.108 g, 0.15 mmol), and KOAc (0.030 g, 0.3 mmol) with $Pd(OAc)_2$ (0.0016 g, 0.007 mmol) in DMAc (3 mL) at 100 °C during 40 h affords the product **4d** in 71% (0.088 g) isolated yield as a brown solid. ^{1}H NMR (500 MHz, $CDCl_3$): δ 8.56 (d, J = 5.6 Hz, 1H), 8.52 (d, J = 5.6 Hz, 1H), 7.88 (t, J = 7.5 Hz, 2H), 7.79−7.74 (m, 2H), 7.63−7.54 (m, 3H), 7.53 (d, J = 8.5 Hz, 2H), 7.18 (t, J = 6.5 Hz, 1H), 7.16−7.05 (m, 2H), 6.94−6.82 (m, 4H), 6.77 (t, J = 7.3 Hz, 1H), 6. 73 (t, J = 7.3 Hz, 1H), 6.34 (d, J = 7.5 Hz, 1H), 6.27 (d, J = 7.5 Hz, 1H), 6.19 (s, 1H), 3.83 (s, 3H). ^{13}C NMR (125 MHz, $CDCl_3$): δ 175.6, 168.4, 168.3, 166.3 (q, J = 31.8 Hz), 160.0, 150.4, 147.9, 147.8, 145.3, 144.8, 144.7, 143.6, 137.3, 137.2, 133.3, 133.2, 130.0, 129.0, 128.9, 127.3, 126.6, 125.5, 123.8, 123.7, 123.1, 121.8, 121.7, 121.1, 121.0, 119.9 (q, J = 273.0 Hz), 118.6, 118.5, 114.4, 92.4, 55.4. HRMS calcd for M^+Na^+ $C_{37}H_{26}N_2O_3F_3NaSIr$ 889.0906, found 889.0904.

dx.doi.org/10.1021/ic401208p | *Inorg. Chem.* 2013, 52, 12416−12428

*Arylation of **4** with 4-Iodoaniline (**4e**).* The reaction of 4-iodoaniline (0.065 g, 0.3 mmol), **4** (0.108 g, 0.15 mmol), and KOAc (0.030 g, 0.3 mmol) with $Pd(OAc)_2$ (0.0016 g, 0.007 mmol) in DMAc (3 mL) at 100 °C during 40 h affords the product **4e** in 70% (0.086 g) isolated yield as a brown solid. ^{1}H NMR (500 MHz, $CDCl_3$): δ 8.56 (d, J = 5.7 Hz, 1H), 8.52 (d, J = 5.7 Hz, 1H), 7.90−7.83 (m, 2H), 7.79−7.70 (m, 2H), 7.63−7.55 (m, 3H), 7.39 (d, J = 7.2 Hz, 2H), 7.17 (t, J = 6.5 Hz, 1H), 7.12 (t, J = 6.5 Hz, 1H), 7.06 (d, J = 3.8 Hz, 1H), 6.90 (t, J = 7.8 Hz, 1H), 6.85 (t, J = 7.8 Hz, 1H), 6.77 (t, J = 7.4 Hz, 1H), 6. 73 (t, J = 7.4 Hz, 1H), 6.62 (d, J = 7.4 Hz, 2H), 6.34 (d, J = 7.6 Hz, 1H), 6.27 (d, J = 7.6 Hz, 1H), 6.18 (s, 1H), 3.80 (s, 2H). ^{13}C NMR (125 MHz, $CDCl_3$): δ 175.7, 168.4, 168.3, 165.9 (q, J = 32 Hz), 151.5, 148.0, 147.9, 147.1, 145.5, 144.8, 144.7, 142.7, 137.3, 137.2, 135.8, 133.3, 133.2, 130.1, 129.0, 128.9, 127.2, 125.5, 123.8, 123.7, 121.8, 121.7, 121.1, 121.0, 120.0 (q, J = 273.0 Hz), 118.6, 118.5, 115.2, 115.1, 92.2. HRMS calcd for M^+Na^+ $C_{36}H_{25}N_3O_2F_3NaSIr$ 836.1141, found 836.1148.

*Arylation of **4** with 2-Chloro-4-iodoaniline (**4f**).* The reaction of 2-chloro-4-iodoaniline (0.076 g, 0.3 mmol), **4** (0.108 g, 0.15 mmol), and KOAc (0.030 g, 0.3 mmol) with $Pd(OAc)_2$ (0.0016 g, 0.007 mmol) in DMAc (3 mL) at 100 °C during 24 h affords the product **4f** in 42% (0.054 g) isolated yield as a brown solid. ^{1}H NMR (500 MHz, $CDCl_3$): δ 8.55 (d, J = 5.6 Hz, 1H), 8.51 (d, J = 5.6 Hz, 1H), 7.92−7.85 (m, 2H), 7.81−7.72 (m, 2H), 7.63−7.55 (m, 3H), 7.50 (d, J = 1.8 Hz, 1H), 7.30−7.25 (m, 1H), 7.18 (t, J = 7.0 Hz, 1H), 7.13 (t, J = 7.0 Hz, 1H), 7.06 (d, J = 4.0 Hz, 1H), 6.90 (t, J = 7.5 Hz, 1H), 6.86 (t, J = 7.5 Hz, 1H), 6.77 (t, J = 7.5 Hz, 1H), 6. 75−6.69 (m, 2H), 6.33 (d, J = 7.5 Hz, 1H), 6.26 (d, J = 7.5 Hz, 1H), 6.17 (s, 1H), 4.19 (s, 2H). ^{13}C NMR (125 MHz, $CDCl_3$): δ 175.5, 168.4, 168.3, 166.1 (q, J = 32.0 Hz), 149.7, 147.9, 147.8, 145.4, 144.8, 144.7, 143.5, 143.2, 137.3, 137.2, 133.3, 133.2, 129.9, 129.0, 128.9, 126.8, 125.6, 125.2, 123.8, 123.7, 122.8, 121.8, 121.6, 121.1, 121.0, 119.5, 118.6, 118.5, 115.8, 92.4. HRMS calcd for M^+Na^+ $C_{36}H_{24}O_2N_3ClF_3NaSIr$ 870.0751, found 870.0745.

Theoretical Calculations. To perform our simulations, we have selected the Gaussian program.[22] The ab initio simulations consisted in geometry optimization and subsequent TD-DFT calculations of the different structures. We have performed default procedures, integration grids, algorithms and parameters, except for tighten energy (1×10^{-9} a.u.) and internal forces (1×10^{-5} a.u.) convergence thresholds and ultrafine integration DFT grid. The ground-state geometrical parameters have been determined with the M06 functional that is known to be efficient for organometallic derivatives.[14] In addition, we have performed a series of benchmark calculations with several hybrid functionals and M06 emerged as efficient for reproducing the XRD distances. Indeed, for **3a** (**3c**), M06 yields Ir−C, Ir−N, and Ir−O bond lengths of 1.980 (1.979), 2.068 (2.068), and 2.155 (2.155) Å, all within 0.01−0.02 Å of the experiment (see Table 1). The vibrational spectrum of each molecule has been subsequently determined analytically at the same level of theory and it has been checked that all structures correspond to true minima of the potential energy surface. At least, the first fourty low-lying excited states have been determined within the vertical TD-DFT approximation using the same functional, that again is pertinent for absorption spectra modeling.[15] For all atoms, we have used the LanL2DZ(5d,7f) basis set and pseudopotential augmented by additional d (C, N, O, S) and f (Ir) functions of contraction length one (α = 0.938, 0.587, 0.736, 0.961, and 0.496 for C, N, O, S, and Ir, respectively). During all steps, a modeling of bulk solvent effects (here CH_2Cl_2) through the polarizable continuum model (PCM) has been applied.[23]

■ ASSOCIATED CONTENT

Supporting Information

^{1}H and ^{13}C NMR spectra and electrochemical data of complexes. This material is available free of charge via the Internet at http://pubs.acs.org.

■ AUTHOR INFORMATION

Corresponding Authors

*E-mail: Denis.Jacquemin@univ-nantes.fr.

*E-mail: henri.doucet@univ-rennes1.fr. Tel: (+33)2-23-23-63-84.

*E-mail: veronique.guerchais@univ-rennes1.fr.

Author Contributions

‡The manuscript was written through contributions of all authors. All authors have given approval to the final version of the manuscript. Authors K.B. and M.Z. contributed equally.

Notes

The authors declare no competing financial interest.

■ ACKNOWLEDGMENTS

Special thanks to Dr. Rémi Métivier (ENS-Cachan) for helping in recording luminescence data. K.B. is grateful to the CNRS and "Région Bretagne" for a PhD grant. This work was supported by LEA CNRS MMC Rennes-Durham. D.J. acknowledges the European Research Council and the *Région des Pays de la Loire* for financial support in the framework of a Starting Grant (Marches -278845) and a *recrutement sur poste stratégique*, respectively. This research used resources of (1) the GENCI-CINES/IDRIS (Grant c2012085117), (2) the CCIPL (*Centre de Calcul Intensif des Pays de Loire*), (3) a local Troy cluster. M. Bonneau and J. Boixel are gratefully acknowledged for recording cyclic voltammetry.

■ REFERENCES

(1) (a) Diederich, F.; Stang, P. J. *Metal-Catalyzed Cross-Coupling Reactions*, Wiley-VCH, New York, 2004. (b) Beller, M.; Bolm, C. *Transition Metals for Organic Synthesis*, 2nd ed.; Wiley−VCH: Weinheim, Germany, 2004. (c) Tsuji, J. *Palladium Reagents and Catalysts*, 2nd ed., Wiley-VCH, New York, 2004. (d) Negishi, E.-I. *Handbook of Organopalladium Chemistry for Organic Synthesis*; Wiley−VCH: New York, 2002. (e) Li, J. J.; Gribble, G. W. *Palladium in Heterocyclic Chemistry*; Pergamon: Amsterdam, 2000.

(2) (a) Akita, Y.; Inoue, A.; Yamamoto, K.; Ohta, A. *Heterocycles* **1985**, *23*, 2327−2333. (b) Ohta, A.; Akita, Y.; Ohkuwa, T.; Chiba, M.; Fukunaga, R.; Miyafuji, A.; Nakata, T.; Tani, N.; Aoyagi, Y. *Heterocycles* **1990**, *31*, 1951−1958.

(3) For reviews, see: (a) Alberico, D.; Scott, M. E.; Lautens, M. *Chem. Rev.* **2007**, *107*, 174−238. (b) Seregin, I. V.; Gevoryan, V. *Chem. Soc. Rev.* **2007**, *36*, 1173−1193. (c) Satoh, T.; Miura, M. *Chem. Lett.* **2007**, *36*, 200−205. (d) Li, B.-J.; Yang, S.-D.; Shi, Z.-J. *Synlett* **2008**, 949−957. (e) Ackermann, L.; Vicente, R.; Kapdi, A. *Angew. Chem., Int. Ed.* **2009**, *48*, 9792−9826. (f) Bellina, F.; Rossi, R. *Tetrahedron* **2009**, *65*, 10269−10310. (g) Roger, J.; Gottumukkala, A. L.; Doucet, H. *ChemCatChem* **2010**, *2*, 20−40. (h) Chen, X.; Engle, K. M.; Wang, D.-H.; Yu, J.-Q. *Angew. Chem., Int. Ed.* **2009**, *48*, 5094−5115. (i) Kuhl, N.; Hopkinson, M. N.; Wencel-Delord, J.; Glorius, F. *Angew. Chem., Int. Ed.* **2012**, *51*, 10236−10254. (j) Wencel-Delord, J.; Glorius, F. *Nat. Chem.* **2013**, *5*, 369−375.

(4) For a selection of palladium-catalysed direct arylations of heteroaromatics with aryl halides, see: (a) Okazawa, T.; Satoh, T.; Miura, M.; Nomura, M. *J. Am. Chem. Soc.* **2002**, *124*, 5286−5287. (b) Masui, K.; Ikegami, H.; Mori, A. *J. Am. Chem. Soc.* **2004**, *126*, 5074−5075. (c) Lanes, B. S.; Sames, D. *Org. Lett.* **2004**, *6*, 2897−2900. (d) Parisien, M.; Valette, D.; Fagnou, K. *J. Org. Chem.* **2005**, *70*, 7578−7584. (e) Zhuralev, F. A. *Tetrahedron Lett.* **2006**, *47*, 2929−2932. (f) Bellina, F.; Cauteruccio, S.; Mannina, L.; Rossi, R.; Viel, S. *J. Org. Chem.* **2005**, *70*, 3997−4005. (g) Cerna, I.; Pohl, R.; Klepetárová, B.; Hocek, M. *Org. Lett.* **2006**, *10*, 5389−5392. (h) Bellina, F.; Cauteruccio, S.; Rossi, R. *Eur. J. Org. Chem.* **2006**, 1379−1382. (i) Martins, A.; Alberico, D.; Lautens, M. *Org. Lett.* **2006**, *8*, 4827−4829. (j) Chiong, H. A.; Daugulis, O. *Org. Lett.* **2007**, *9*, 1449−1459.

(k) Martins, A.; Lautens, M. *J. Org. Chem.* **2008**, *73*, 8705−8710. (l) Yanagisawa, S.; Ueda, K.; Sekizawa, H.; Itami, K. *J. Am. Chem. Soc.* **2009**, *131*, 14622−14623. (m) Liegault, B.; Petrov, I.; Gorelsky, S. I.; Fagnou, K. *J. Org. Chem.* **2010**, *75*, 1047−1060. (n) Ohnmacht, S. A.; Culshaw, A. J.; Greaney, M. F. *Org. Lett.* **2010**, *12*, 224−226. (o) Schipper, D. J.; Fagnou, K. *Chem. Mater.* **2011**, *23*, 1594−1600. (p) Nadres, E. T.; Lazareva, A.; Daugulis, O. *J. Org. Chem.* **2011**, *76*, 471−483. (q) Dröge, T.; Notzon, A.; Fröhlich, R.; Glorius, F. *Chem.—Eur. J.* **2011**, *17*, 11974−11977.

(5) Selected recent contributions from our laboratories: (a) Roger, J.; Požgan, F.; Doucet, H. *Adv. Synth. Catal.* **2010**, *352*, 696−710. (b) Chen, L.; Roger, J.; Bruneau, C.; Dixneuf, P. H.; Doucet, H. *Chem. Commun.* **2011**, *47*, 1872−1874. (c) Roy, D.; Mom, S.; Lucas, D.; Cattey, H.; Hierso, J.-C.; Doucet, H. *Chem.—Eur. J.* **2011**, *17*, 6453−6461. (d) Si Larbi, K.; Fu, H. Y.; Laidaoui, N.; Beydoun, K.; Miloudi, M.; El Abed, D.; Djebbar, S.; Doucet, H. *ChemCatChem* **2012**, *4*, 815−823. (e) Beydoun, K.; Roger, J.; Boixel, J.; Le Bozec, H.; Guerchais, V.; Doucet, H. *Chem. Commun.* **2012**, *48*, 11951−11953. (f) Fu, H. Y.; Chen, L.; Doucet, H. *J. Org. Chem.* **2012**, *77*, 4473−4478.

(6) (a) Liu, Z.; Bian, Z.; Huang, C. In *Molecular Organometallic Materials for Optics*, Le Bozec, H.; Guerchais, V., Eds.; Topics in Organometallic Chemistry; Springer: Heidelberg, Germany, 2010; Vol. *28*, pp 113; (b) You, Y.; Nam, W. *Chem. Soc. Rev.* **2012**, *41*, 7061−7084.

(7) For examples of iridium tris-cyclometalated complexes: (a) Baldo, M. A.; O'Brien, D. F.; You, Y.; Shoustikov, A.; Sibley, S.; Thompson, M. E.; Forrest, S. R. *Nature* **1998**, *395*, 151−154. (b) Grushin, V. V.; Herron, N.; LeCloux, D. D.; Marshall, W, J.; Petrov, V. A.; Wang, Y. *Chem. Commun.* **2001**, *16*, 1494−1495. (c) Tsuboyama, A.; Iwawaki, H.; Furugori, M.; Mukaide, T.; Kamatani, J.; Igawa, S.; Moriyama, T.; Miura, S.; Takiguchi, T.; Okada, S.; Hoshino, M.; Ueno, K. *J. Am. Chem. Soc.* **2003**, *125*, 12971−12979. (d) Tamayo, A. B.; Alleyne, B. D.; Djurovich, P. I.; Lamansky, S.; Tsyba, I.; Ho, N. N.; Bau, R.; Thompson, M. E. *J. Am. Chem. Soc.* **2003**, *125*, 7377−7387. (e) Lepeltier, M.; Le Bozec, H.; Guerchais, V.; Lee, T. K.-M.; Lo, K. K.-W. *Organometallics* **2005**, *24*, 6069−6072. (f) Kuil, J.; Steunenberg, P.; Chin, P. T. K.; Oldenburg, J.; Jalink, K.; Velders, A. H.; van Leeuwen, F. W. B. *ChemBioChem.* **2011**, *12*, 1897−1903.

(8) For examples of iridium bis-cyclometallated complexes: (a) Lamansky, S.; Djurovich, P.; Murphy, D.; Abdel-Razzaq, F.; Lee, H.-E.; Adachi, C.; Burrows, P. E.; Forrest, S. R.; Thompson, M. E. *J. Am. Chem. Soc.* **2001**, *123*, 4304−4312. (b) Lamansky, S.; Djurovich, P.; Murphy, D.; Abdel-Razzaq, F.; Kwong, R.; Tsyba, I.; Bortz, M.; Mui, B.; Bau, R.; Thompson, M. E. *Inorg. Chem.* **2001**, *40*, 1704−1711. (c) Xu, M. L.; Wang, G. Y.; Zhou, R.; An, Z. W.; Zhou, Q.; Li, W. L. *Inorg. Chim. Acta* **2007**, *360*, 3149−3154. (d) Kozhevnikov, D. N.; Kozhevnikov, V. N.; Shafikov, M. Z.; Prokhorov, A. M.; Bruce, D. W.; Williams, J. A. G. *Inorg. Chem.* **2011**, *50*, 3804−3815.

(9) Examples of Negishi or Suzuki couplings on iridium complexes have been reported: see, inter alia: (a) Fang, Y. G.; Polson, M. I. J.; Hanan, G. S. *Inorg. Chem.* **2003**, *42*, 5−7. (b) Arm, K. J.; Williams, J. A. G. *Chem. Commun.* **2005**, 230−232.

(10) Beydoun, K.; Zaarour, M.; Williams, J. A. G.; Doucet, H.; Guerchais, V. *Chem. Commun.* **2012**, *48*, 1260−1262.

(11) (a) You, Y.; Park, S. Y. *J. Am. Chem. Soc.* **2005**, *127*, 12438−12439. (b) Baranoff, E.; Jung, I.; Scopelliti, R.; Solari, E.; Grätzel, M.; Nazeeruddin, M. K. *Dalton Trans.* **2011**, *40*, 6860−6867.

(12) Yu, T.; Yang, S.; Meng, J.; Zhao, Y.; Zhang, H.; Fan, D.; Han, X.; Liu, Z. *Inorg. Chem. Commun.* **2011**, *14*, 159−161.

(13) Zhao, Q.; Jiang, C.-Y.; Shi, M.; Li, F.-Y.; Yi, T.; Cao, Y.; Huang, C.-H. *Organometallics* **2006**, *25*, 3631−3638.

(14) Zhao, Y.; Truhlar, D. G. *Theor. Chem. Acta* **2008**, *120*, 215−241.

(15) (a) Jacquemin, D.; Perpète, E. A.; Ciofini, I.; Adamo, C.; Valero, R.; Zhao, Y.; Truhlar, D. G. *J. Chem. Theory Comput.* **2010**, *6*, 2071−2085. (b) Jacquemin, D.; Planchat, A.; Adamo, C.; Mennucci, B. *J. Chem. Theory Comput.* **2012**, *8*, 2359−2372.

(16) (a) Chen, Y.-L.; Li, S.-W.; Chi, Y.; Cheng, Y.-M.; Pu, S.-C.; Yeh, Y.-S.; Chou, P.-T. *ChemPhysChem* **2005**, *6*, 2012−2017. (b) Chou, P.-T.; Chi, Y.; Chung, M.-W.; Lin, C.-C. *Coord. Chem. Rev.* **2011**, *255*, 2653.

(17) Yersin, H.; Rausch, A. F.; Czerwieniec, R.; Hofbeck, T.; Fischer, T. *Coord. Chem. Rev.* **2011**, *255*, 2622.

(18) Nakamaru, K. *Bull. Chem. Soc. Jpn.* **1982**, *55*, 2697−2705.

(19) (a) Sheldrick, G. M. *SAINT*; Bruker AXS: Madison, WI, 2006; (b) Sheldrick, G. M. *SADABS*; Bruker AXS: Madison, WI, 2006.

(20) Altomare, A.; Burla, M. C.; Camalli, M.; Cascarano, G.; Giacovazzo, C.; Guagliardi, A.; Moliterni, A. G. G.; Polidori, G.; Spagna, R. *J. Appl. Crystallogr.* **1999**, *32*, 115−119.

(21) Sheldrick, G. M. *Acta Crystallogr., Sect. A* **2008**, *64*, 112−122.

(22) Frisch, M. J.; Trucks, G. W.; Schlegel, H. B.; Scuseria, G. E.; Robb, M. A.; Cheeseman, J. R.; Scalmani, G.; Barone, V.; Mennucci, B.; Petersson, G. A.; Nakatsuji, H.; Caricato, M.; Li, X.; Hratchian, H. P.; Izmaylov, A. F.; Bloino, J.; Zheng, G.; Sonnenberg, J. L.; Hada, M.; Ehara, M.; Toyota, K.; Fukuda, R.; Hasegawa, J.; Ishida, M.; Nakajima, T.; Honda, Y.; Kitao, O.; Nakai, H.; Vreven, T.; Montgomery, Jr., J. A.; Peralta, J. E.; Ogliaro, F.; Bearpark, M.; Heyd, J. J.; Brothers, E.; Kudin, K. N.; Staroverov, V. N.; Kobayashi, R.; Normand, J.; Raghavachari, K.; Rendell, A.; Burant, J. C.; Iyengar, S. S.; Tomasi, J.; Cossi, M.; Rega, N.; Millam, J. M.; Klene, M.; Knox, J. E.; Cross, J. B.; Bakken, V.; Adamo, C.; Jaramillo, J.; Gomperts, R.; Stratmann, R. E.; Yazyev, O.; Austin, A. J.; Cammi, R.; Pomelli, C.; Ochterski, J. W.; Martin, R. L.; Morokuma, K.; Zakrzewski, V. G.; Voth, G. A.; Salvador, P.; Dannenberg, J. J.; Dapprich, S.; Daniels, A. D.; Farkas, Ö.; Foresman, J. B.; Ortiz, J. V.; Cioslowski, J.; Fox, D. J. *Gaussian 09*, Revision C.01; Gaussian Inc.: Wallingford, CT, 2009.

(23) Tomasi, J.; Mennucci, B.; Cammi, R. *Chem. Rev.* **2005**, *105*, 2999−3094.